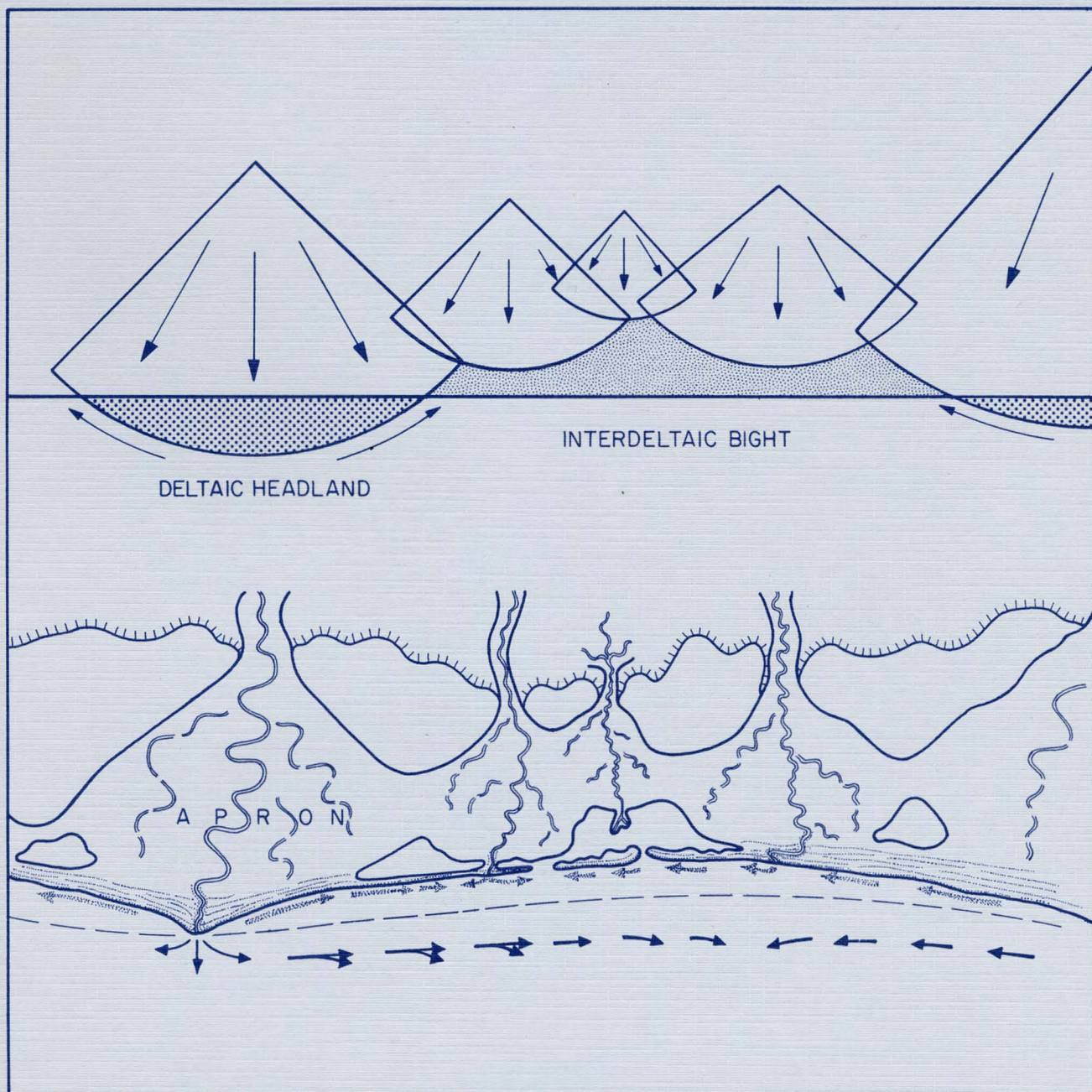


# Lower Miocene (Fleming) Depositional Episode of the Texas Coastal Plain and Continental Shelf: Structural Framework, Facies, and Hydrocarbon Resources

William E. Galloway,  
Lee A. Jirik,  
Robert A. Morton,  
and Jules R. DuBar



**Bureau of Economic Geology • W. L. Fisher, Director**

The University of Texas at Austin • Austin, Texas 78713

1986



Report of Investigations No. 150

# **Lower Miocene (Fleming) Depositional Episode of the Texas Coastal Plain and Continental Shelf: Structural Framework, Facies, and Hydrocarbon Resources**

William E. Galloway,  
Lee A. Jirik,  
Robert A. Morton,  
and Jules R. DuBar

assisted by

Emil Bramson and Charles E. Yager

Research supported by the Minerals Management Service, U.S. Department of the Interior,  
under agreement nos. 14-12-0001-30115 and 14-12-0002-40029.



**Bureau of Economic Geology • W. L. Fisher, Director**

The University of Texas at Austin • Austin, Texas 78713

1986







# CONTENTS

<b>Abstract</b> .....	1
<b>Introduction</b> .....	1
Stratigraphic nomenclature and zonation .....	2
Depositional setting .....	4
Episode boundaries, correlation, and operational map units .....	6
Objectives .....	10
<b>Structural Framework</b> .....	11
Reactivated structures .....	11
Contemporaneous structures .....	11
<b>Lower Miocene Depositional Framework</b> .....	14
Sources of data .....	14
Lower Miocene depositional systems .....	19
Santa Cruz fluvial system .....	19
North Padre delta system .....	22
Moulton/Point Blank streamplain .....	23
Matagorda barrier/strandplain system .....	23
Newton fluvial system .....	24
Calcasieu delta system .....	25
Depositional history and paleogeography .....	26
<b>Origin and Distribution of Hydrocarbons</b> .....	30
Indigenous source rocks and maturation history .....	30
Migration and entrapment .....	31
Occurrence of oil and gas .....	32
General features of lower Miocene plays .....	32
Exploration potential .....	39
Onshore and State submerged lands .....	39
Outer Continental Shelf .....	39
<b>Conclusions</b> .....	41
<b>Acknowledgments</b> .....	42
<b>References</b> .....	43
<b>Appendix: Tabulation of fields by play</b> .....	45

## Figures

1. Gulf Coast Cenozoic depositional episodes .....	3
2. Lithostratigraphic and biostratigraphic subdivision of the lower Miocene section, Northwest Shelf of the Gulf of Mexico .....	4
3. Index map and depositional framework of the lower Miocene (Fleming) depositional episode .....	5
4. Schematic reconstruction of the stratigraphic architecture of a Gulf Coast Cenozoic depositional sequence .....	7
5. Electric log response of typical facies sequences within the depositional complex of a Gulf Coast Cenozoic episode .....	9
6. Schematic cross section of the lower Miocene depositional sequence, Texas Coastal Plain and shelf, showing the lithostratigraphic and biostratigraphic features used for correlation .....	10



7. Structural framework of the lower Miocene sequence .....	12
8. Net-sandstone isopach map of the Oakville (Anahuac shale to <i>Marginulina a.</i> ) operational unit .....	15
9. Percent-sandstone map of the Oakville (Anahuac shale to <i>Marginulina a.</i> ) operational unit .....	16
10. Net-sandstone isopach map of the Lagarto ( <i>Marginulina a.</i> to <i>Amphistegina B</i> shale) operational unit .....	17
11. Percent-sandstone map of the Lagarto ( <i>Marginulina a.</i> to <i>Amphistegina B</i> shale) operational unit .....	18
12. Generalized paleobathymetry of Oakville and Lagarto map interval mudstones .....	20
13. Lower Miocene depositional systems and their component elements .....	21
14. Paleogeographic reconstruction during later Oakville progradation and middle Lagarto coastal plain aggradation .....	27
15. Interpretive morphologic profiles across the lower Miocene coastal plain, shoreline, shelf, and slope .....	28
16. Depositional architecture of the lower Miocene coastal plain and shoreline .....	29
17. Distribution of lower Miocene oil and gas fields that have produced more than 1 million boe of hydrocarbons .....	33
18. Cumulative oil and gas production for each of the nine lower Miocene plays .....	37
19. Total hydrocarbon yield factors calculated on the basis of estimated total rock volume and total sandstone volume contained within each of the nine Miocene plays .....	37
20. Distribution of total producible reserves in 32 Miocene fields in Federal OCS areas .....	41

## Tables

1. Total organic carbon content of lower Miocene mudstones .....	31
2. Summary of geologic characteristics and remaining potential of lower Miocene oil and gas plays .....	34
3. Cumulative production and sedimentary volumes of lower Miocene plays .....	38
4. Projected volumes of undiscovered recoverable hydrocarbons .....	40

## Plates (in pocket)

- I. Structural cross section 1-1'
- II. Structural cross section 12-12'
- III. Structural cross section 19-19'
- IV. Net-sandstone isopach map, Oakville operational unit
- V. Percent-sandstone map, Oakville operational unit
- VI. Net-sandstone isopach map, Lagarto operational unit
- VII. Percent-sandstone map, Lagarto operational unit

## ABSTRACT

The Fleming Group and its basinward equivalents constitute the stratigraphic record of one of the major Cenozoic depositional episodes of the northern Gulf Coast Basin. The depositional sequence representing the episode is bounded above by the *Amphistegina* B shale and below by the Anahuac shale. Initially, lower Miocene (Oakville) progradation advanced across the broad submerged shelf platform constructed during earlier Frio deposition. When outbuilding reached the Frio paleocontinental margin, the rate slowed as large-scale growth faulting created a narrow lower Miocene expansion zone. The later portion of the lower Miocene episode, generally equivalent to the Lagarto Formation, was characterized by long-term shoreline stability and retreat punctuated by local, temporary progradation.

In South Texas, the lower Miocene depositional framework includes the Santa Cruz fluvial system and the North Padre delta system. The bed-load fluvial complex fed a wave-dominated delta, constructing a broadly convex deltaic headland across the foundered Frio Norias delta system. Extensive wave reworking and longshore transport of sand and mud nourished a broad barrier-island/lagoon and strandplain complex that extended along the central and much of the northeastern Texas coast. This well-known barrier/strandplain system was bounded updip by a coastal plain traversed by numerous, small, intrabasinal streams. Near the present Sabine River, westernmost deposits of a continental-scale mixed-load fluvial and equivalent delta system extend beneath the Texas Coastal Plain and shelf from the Miocene depocenter in Louisiana. Here, the early phase of lower Miocene progradation was also complicated by the incision and filling of numerous submarine gorges.

Lower Miocene reservoirs have produced nearly 4 billion barrels of oil equivalent of petroleum from nine identified plays in the Texas Coastal Plain and shelf. The most prolific play, the Houston Embayment salt domes, accounts for nearly all the oil and more than two-thirds of the total production from deposits of the episode. Four offshore plays offer the greatest area for discovery of substantial new reserves, primarily of gas. To date, however, the yield per volume of reservoir sandstone for Miocene plays remains low relative to more prolific units, such as the Frio Formation.

**Keywords:** Fleming, Oakville, lower Miocene, petroleum (oil and gas), depositional system

## INTRODUCTION

Numerous major and minor episodes of sediment input and continental platform construction punctuate the Cenozoic depositional history of the Northwest Shelf of the Gulf of Mexico. Frazier (1974), studying the Quaternary section of the Gulf Coast, defined a depositional episode and its physical stratigraphic equivalent, a depositional complex. Each depositional complex consists of many discrete facies sequences, derived

from common sources along the basin margin and deposited during a period of relative base-level stability. The depositional complex of each depositional episode is bounded basinward by transgressive units and hiatal intervals of regional or worldwide significance. Boundaries are ill defined landward of the shoreline of maximum transgression. Depositional episodes are thus informal time-stratigraphic subdivisions of the basin fill that

are generally comparable to the formal diachronic episodes defined in the North American stratigraphic code (North American Commission on Stratigraphic Nomenclature, 1983).

Using this definition, Jackson and Galloway (1984) outlined the principal depositional episodes of the northern Gulf Basin and compared their temporal distribution and relative magnitude of continental margin offlap to the proposed Cenozoic eustatic sea-level curve (fig. 1). The Miocene depositional record exhibits two major progradational pulses separated by a regional transgressive middle Miocene interval, the *Amphistegina* B shale. Both the lower and middle-to-upper Miocene episodes of continental margin offlap extend laterally across several depocenters of the northern Gulf of Mexico (Rainwater, 1964). Their coincidence with inferred early and late Miocene sea-level lowstands suggests extrabasinal influences on deposition, possibly including large-scale plate interactions or eustatic sea-level changes.

The relationship of Gulf Coast deposition to Miocene events in the North American plate is ambiguous. Steepening of Pacific plate subduction during late Oligocene and early Miocene time led to renewed arc volcanism and development of large-scale tensional features in the southern Cordillera (Dickinson, 1981). The Rio Grande rift, the closest prominent manifestation of this tensional stress regime, was actively subsiding during the Miocene. Development of the rift probably would have markedly affected the drainage patterns of the southwestern United States and northern Mexico. The rift would have acted as a focus for drainage elements, funneling a major river southward into West Texas. However, much of the sediment transported by this large drainage axis would have remained trapped within rapidly subsiding parts of the rift, effectively capturing the sediment supply of the Rio Grande Embayment of South Texas. Indeed, the focus of major sediment input and deltaic progradation shifted abruptly from the Rio Grande Embayment to Louisiana between Oligocene and Miocene time (Martin, 1978; Winker, 1982). The decreasing importance of the South Texas depocenter also may have been influenced by the waning of volcanism in

northwestern Mexico (McDowell and Clabaugh, 1979) and by the lull in southern Cordilleran volcanic activity, which extended through middle Miocene time (Chapin, 1979). Finally, uplift of the Edwards Plateau along the Balcones Fault Zone (Weeks, 1945), which is indicated by the flood of reworked Cretaceous sediment and fossils in the Oakville section, may have further isolated the middle and southern Texas Coastal Plain from major continental drainage elements.

By Miocene time, glacial-eustatic changes in sea level had become a potential cause of depositional cyclicity. Antarctic glaciation began during the Oligocene, and an ice cap was forming by Miocene time (Loutit and Kennett, 1981; Leckie and Webb, 1983). Evidence of "refrigeration" of the Gulf of Mexico during the middle Miocene was summarized by Echols and Curtis (1973).

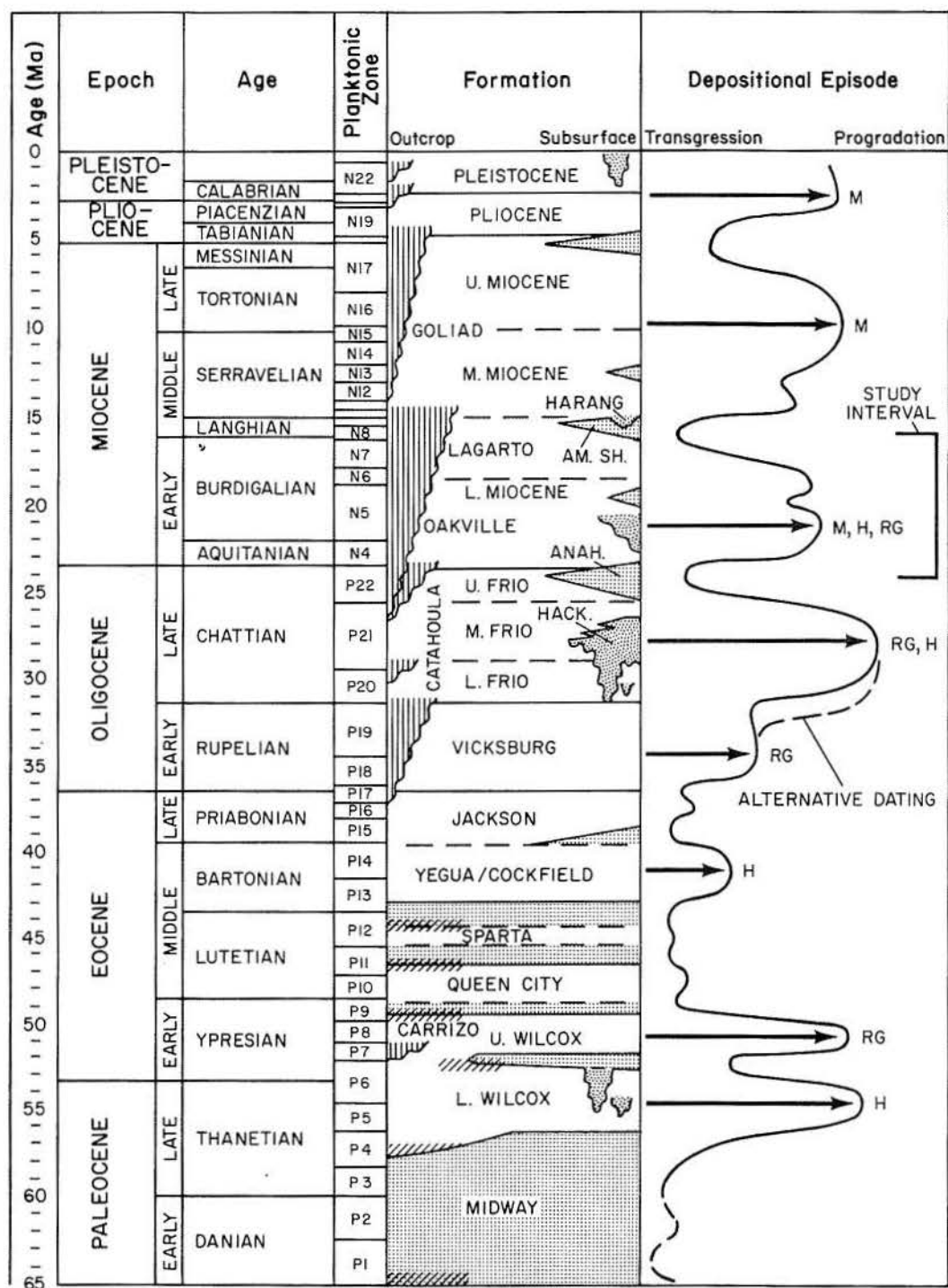
## Stratigraphic Nomenclature and Zonation

The lithostratigraphic nomenclature and biostratigraphic zonation of the lower Miocene depositional episode is shown in figure 2. Equivalent strata at outcrop are included within the Fleming Group as mapped on the Geologic Atlas of Texas (Barnes, 1974). Note that this correlation deviates from the conventional correlations shown on most stratigraphic charts that equate the entire Miocene with the Fleming outcrop. Careful correlation of subsurface units to outcrop (Solis, 1981; Galloway and others, 1982a; Hoel, 1982), as well as dating of contained vertebrate faunas (DuBar, 1983; Tedford and Hunter, 1984), shows that the overlying Goliad Formation is largely middle to late Miocene and not Pliocene as usually indicated.

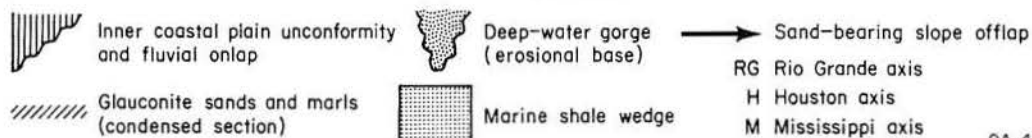
Across the central Texas Coastal Plain, the Fleming Group outcrop is subdivided into the underlying, sandy Oakville Formation and the overlying, comparatively mud-rich Lagarto Formation (figs. 2 and 3). In East Texas and South Texas, the Fleming is undivided (fig. 3).

In the deep subsurface, the Miocene section is in part subdivided by several regional shale tongues, including the bounding Anahuac and *Amphistegina* B shales (fig. 2). Finer subdivision is conventionally based on numerous





#### EXPLANATION



QA 4177

**Figure 1.** Gulf Coast Cenozoic depositional episodes. Principal marine shale tongues, condensed paleontologic zones, and unconformities that delimit the depositional record of the episodes are also indicated. Modified from Jackson and Galloway (1984).

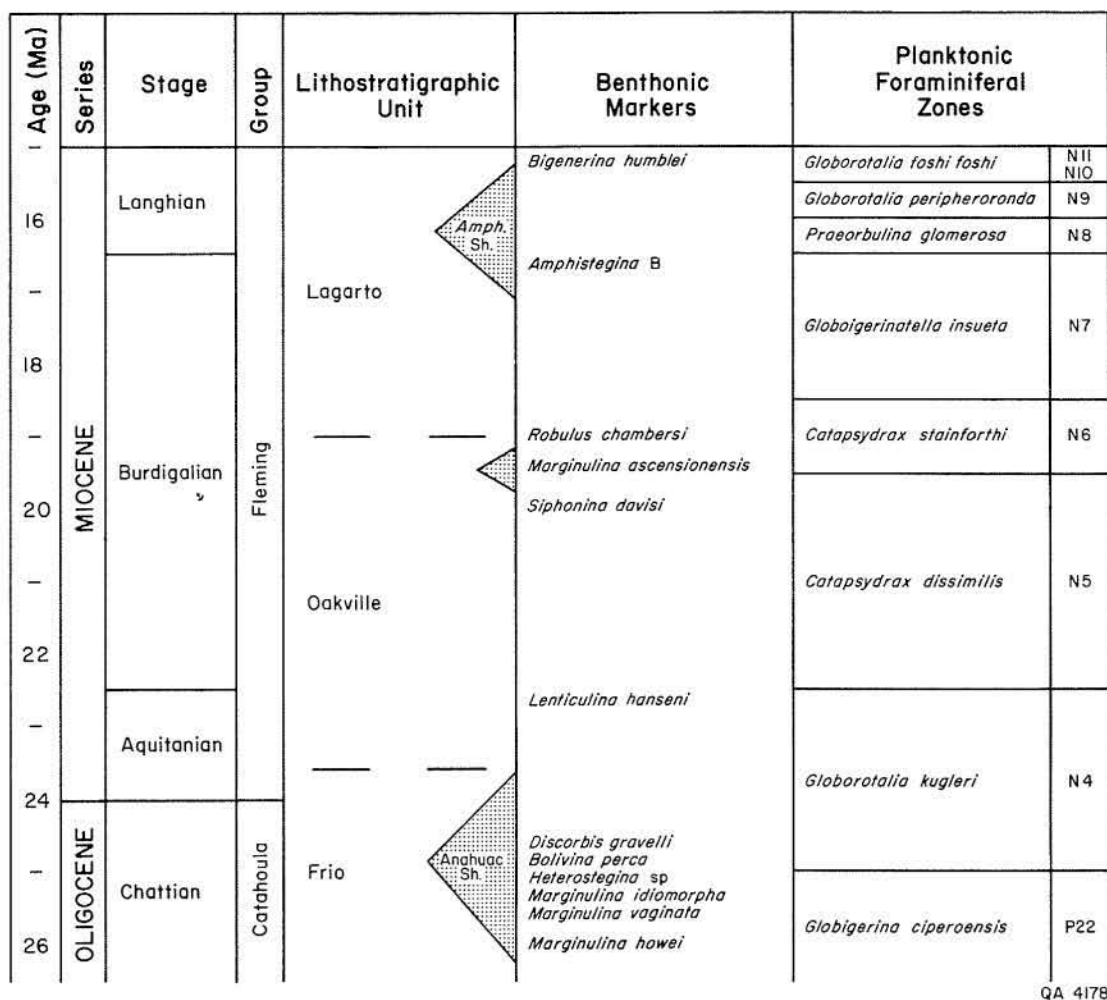


**Figure 2.** Lithostratigraphic and biostratigraphic subdivision of the lower Miocene section, Northwest Shelf of the Gulf of Mexico.

species of benthonic foraminifera. More recently, deep-water sections have been zoned using planktonic foraminifera, allowing accurate dating of the Miocene depositional units and the more commonly used benthonic markers. The lower Miocene depositional episode extended from approximately 16 to 24 mya (fig. 1), encompassing the Aquitanian, Burdigalian, and early Langhian Stages.

## Depositional Setting

The Fleming Group crops out across the inner coastal plain, except in South Texas, where it is overlapped by a veneer of Goliad gravel and caliche (fig. 3). From outcrop, a gently dipping, coastward-thickening section of sands and mudstones extends basinward to the progradational continental margin of the

underlying Frio depositional sequence. Between the updip limit of the Anahuac marine shale and the Frio shelf margin, the lower Miocene systems prograded across a relatively shallow-water depositional shelf platform. Basinward of the Frio paleomargin, the Miocene section thickens dramatically, reflecting progradation of the continental slope. Downdip limits of the lower Miocene depositional complex that have been penetrated by drilling conform closely to the maximum basinward development of the lower Miocene paleomargin. This prograded lower Miocene continental platform, in turn, foundered and was covered by the middle Miocene *Amphistegina B* shale. Maximum updip extent of the *Amphistegina B* shoreline extended to or inland of the present shoreline (fig. 3). The Anahuac and *Amphistegina B*

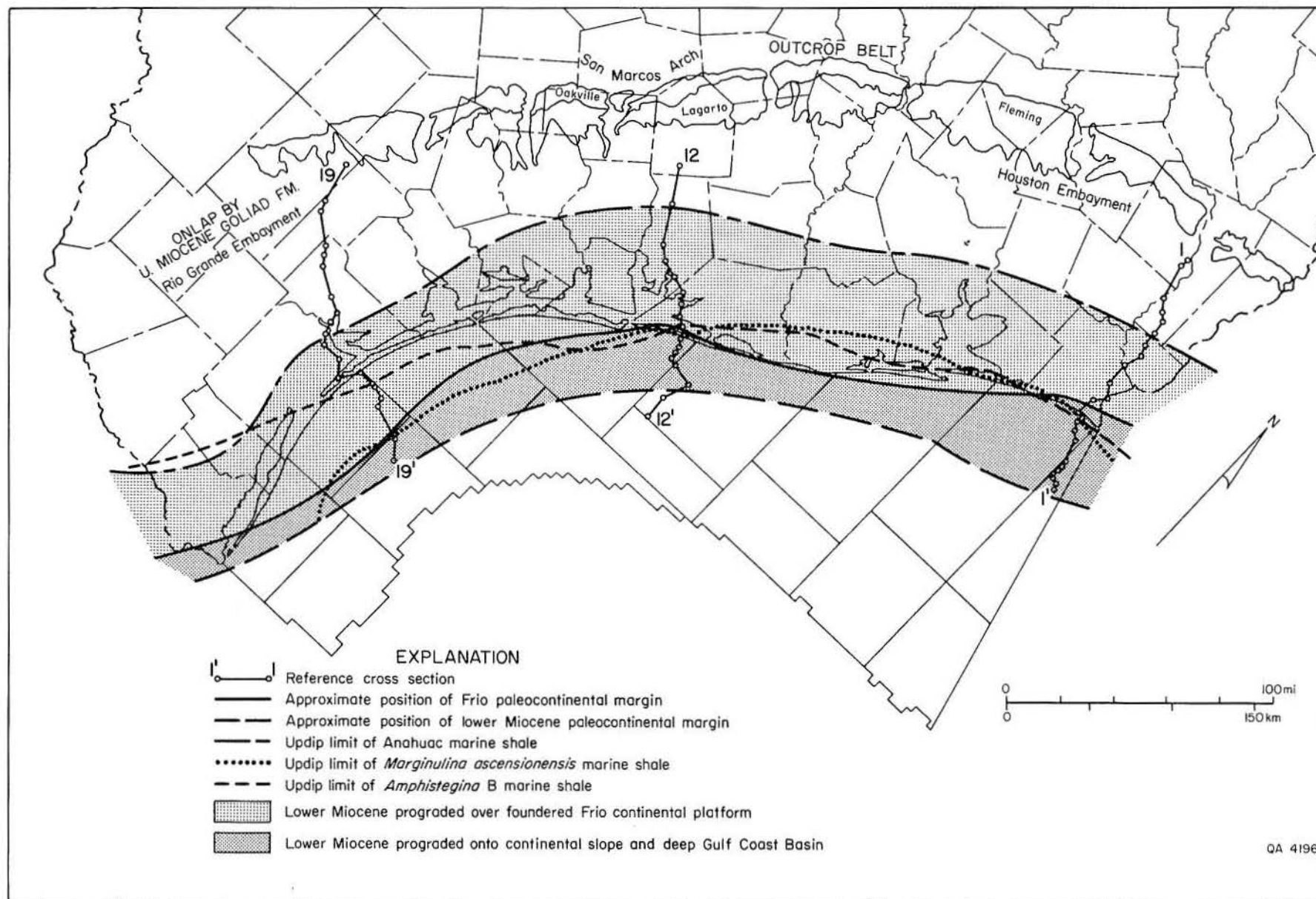


**Figure 3.** Index map and depositional framework of the lower Miocene (Fleming) depositional episode. Reference cross sections are shown in plates 1 through 3. Updip limits of the Anahuac and *Amphistegina* B shales indicate the extent of shoreline retreat before and after the episode of coastal and slope progradation.



shales provide the key stratigraphic boundaries of the lower Miocene depositional episode. Basinward, thick slope and basinal lower Miocene deposits undoubtedly exist, but they are deeply buried beneath the progradational continental platform of the upper Miocene and younger units.

## Episode Boundaries, Correlation, and Operational Map Units

Extensive marine shale wedges, such as the Anahuac and *Amphistegina* B, are regional stratigraphic products of base-level rise, coastal retreat, and continental platform submergence that define Gulf Coast depositional episodes. Extrapolation of episode boundaries updip into the nonmarine section beyond landward limits of transgression and downdip into thick, sand-poor shelf and slope sequences, as well as rational subdivision of episode depositional sequences into thinner map units, requires a conceptual understanding of the dynamics and architecture of Gulf Coast deposition.

Figure 4 schematically illustrates the formation of a major Gulf Coast Cenozoic depositional sequence during an episode such as the lower Miocene. For simplicity, boundaries between depositional increments are shown to be linear. In reality, flexural subsidence induced by depositional loading at the continental margin would produce a more complex pattern of subsidence and peripheral uplift than that shown in figure 4 (Keen and others, 1981; Winker, 1982). The panels in figure 4 highlight important periods in episode evolution:

(1) The terminal inundation of the underlying continental platform (fig. 4a) results in shoreline retreat and retrogradational sedimentation. Compactional and isostatic crustal subsidence increases water depths over the submerged platform, which forms a broad shelf upon which distal shore-zone and shelf sediments accumulate. Landward, the rise in base level and the areal expansion of the surface of sediment and water loading (and resultant subsidence bowl) accentuate aggradation of shoreline and coastal plain deposits. It

is important to note that the depth of the submerged platform, or shelf, may vary greatly depending on relative rates of subsidence, eustatic sea-level change, and sediment supply; the 600-ft (180-m) depth limit typical of modern shelves is the common product of the eustasy-dominated Quaternary interplay of these three factors.

(2) Renewed excess of sediment input over subsidence results in coastal progradation across the submerged shelf platform (fig. 4b). Part of the marine shale wedge is thus genetically related to the depositional complex of this new episode. Rapid basinward advance of the shoreline and a stable or slowly subsiding base level favor preservation of a compressed fluvial section along the inland margin of the depositional complex.

(3) As progradational deposits of the new episode reach the underlying paleocontinental margin, a much thicker prism of sediment is deposited in deep water on the continental slope (fig. 4c). The rate of shoreline advance slows. The offlapping continental margin is the locus of a new generation of tensional faulting, and depositional loading induces flow, intrusion, and diapirism of underconsolidated mud or salt (Winker and Edwards, 1983). Rapid, localized loading of transitional oceanic crust accentuates flexural subsidence and concomitant aggradation of coastal plain sediments. Accelerated basinward subsidence and tilting in response to renewed linear crustal loading along the continental margin may also accentuate slight uplift of the landward margin of the basin fill and result in low-angle truncation of older units and deposition of a fluvial veneer along the inland periphery of the coastal plain, particularly in areas traversed by well-developed fluvial systems.

(4) The terminal base-level rise results in landward retreat of the facies tract and favors aggradation of both shore-zone and coastal plain depositional systems (fig. 4d). Preservation of interchannel fluvial deposits is enhanced, and fluvial sediments may onlap the inner coastal plain erosional surface.

Figure 4e illustrates the composite stratigraphic architecture produced by the depositional episode and locates typical facies sequences shown in figure 5. Along the updip fringe of the depositional complex, the lower

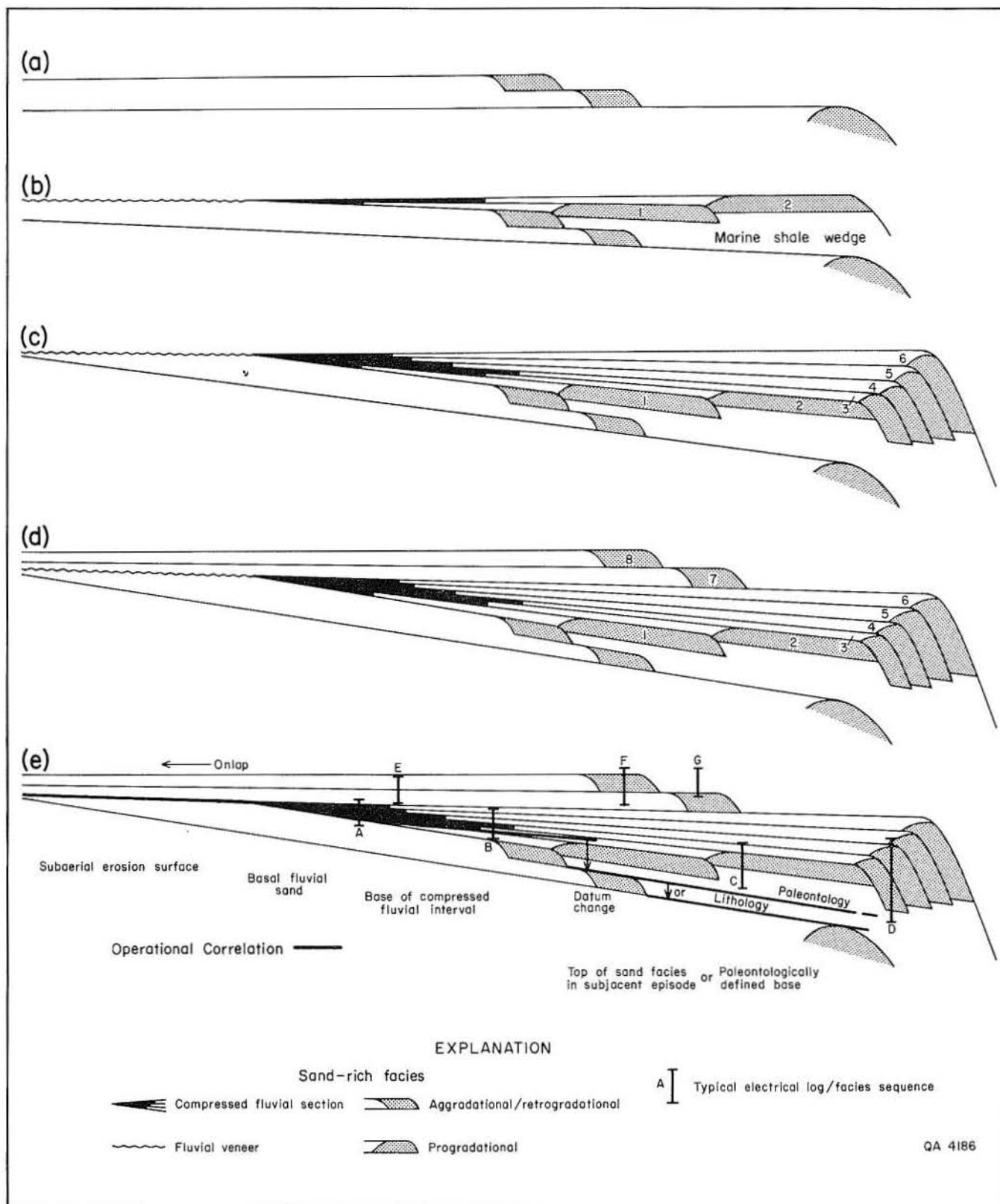


**Figure 4.** Schematic reconstruction of the stratigraphic architecture of a Gulf Coast Cenozoic depositional sequence. (a) Shoreline retreat and marine transgression. (b) Rapid progradation across the foundered continental platform. (c) Slow progradation of the continental margin. (d) Shoreline retreat and coastal plain aggradation. (e) Operational correlation boundaries separating the depositional complexes of successive episodes. See text for additional discussion.

fluvial sequence is characterized by preferential preservation of amalgamated, sandy channel-fill deposits (fig. 5, sequences A and B), which may locally rest on a low-angle truncation surface. Upper sequences typically show greater proportions of muddy inter-channel facies (fig. 5, sequence E). Such a sequence is directly comparable to the subdivision of the Fleming into sand-rich Oakville and mud-rich Lagarto lithostratigraphic units. The alluvial fill of the lower Mississippi Valley reveals a similar facies subdivision, reflecting post-glacial sea-level rise (Fisk, 1944). In mid-dip areas, a complete progradational sequence is capped by thick aggradational shoreline and subaerial coastal plain facies (fig. 5, sequence C). The upper, retrogradational portion of the complex is dominated by aggradational sequences, including thick, coastal plain mudstones and strandline sand bodies (fig. 5, sequence F). Thick sand-rich intervals reflect marine reworking and deposition of sand along the shoreline. Finally, downdip facies sequences exhibit tremendous expansion of progradational strandline, shelf, and upper slope units (fig. 5, sequence D) overlain by marine shelf mudstone, deposited seaward of the gradually retreating shoreline (fig. 5, sequence G).

Figure 4e shows that no single correlation marker bounds the entire depositional episode. The initiation of an episode is marked updip by a basal erosion surface or approximated by the base of the amalgamated fluvial channel sands. This latter boundary climbs section downdip but is the only physical stratigraphic feature that can be realistically correlated in the nonmarine section. Downdip, the bounding marine shale tongue provides several operational correlation points. The top of sands within the underlying depositional complex is a functional lithologic pick that extends to the older paleomargin. Within the shale, a paleontologic marker that approximates the change from retrogradational to renewed progradational deposition is perhaps the ideal genetic boundary. A shift from benthonic to planktonic faunas is required for correlation basinward of the older paleomargin, but few wells penetrate these deeply buried slope equivalents. Thus, inherent in depositional episode stratigraphic architecture is the

operational necessity for an arbitrary shift in the bounding datum if correlation and mapping are to be extended updip beyond the bounding marine shales. Boundaries of the top of the episode sequence are, of course, the lower boundaries of the depositional complex introduced by the subsequent depositional episode.

Operational boundaries used for regional mapping of the lower Miocene depositional complex are shown in figure 6. Beginning at the outcrop, the base of massive Oakville Sandstone is traced or projected basinward to the updip limit of the Anahuac shale. The correlation datum then drops to the top of the highest Frio sandstone and continues downdip until adequate paleontologic control is available. In thicker shale sections, the first occurrence of *Bolivina perca* provides a widespread marker that approximates the lower episode boundary. The base of massive Goliad sands similarly defines the updip top of the Fleming depositional episode. The datum is then lowered to the stratigraphic position of the first occurrence of *Amphistegina* B within the overlying shale wedge.

The depositional sequence so defined is several thousand feet thick along its basinward margin. To improve paleogeographic resolution, the lower Miocene has further been subdivided into two operational map units. The lower unit (A) corresponds to the Oakville Sandstone of the shallow subsurface and to the dominantly progradational pre-*Marginulina ascensionensis* deposits at depth (fig. 6). The upper unit (B) consists of dominantly aggradational fluvial and retrogradational coastal deposits of the upper part of the episode. The *Marginulina* a. transgressive shale provides a widespread stratigraphic marker that extends nearly as far updip as does the *Amphistegina* B shale over most of the study area (fig. 3). Brackish-water deposits, which contain oysters and are found in the middle Fleming outcrop near Burkeville (Newton County) and in adjacent Louisiana parishes (Stenzel and others, 1944; Floyd and others, 1958), most likely are updip equivalents of this mid-episode transgression.

Twenty-four dip and four strike cross sections, based on those of Dodge and Posey (1981) and their offshore extensions (Morton



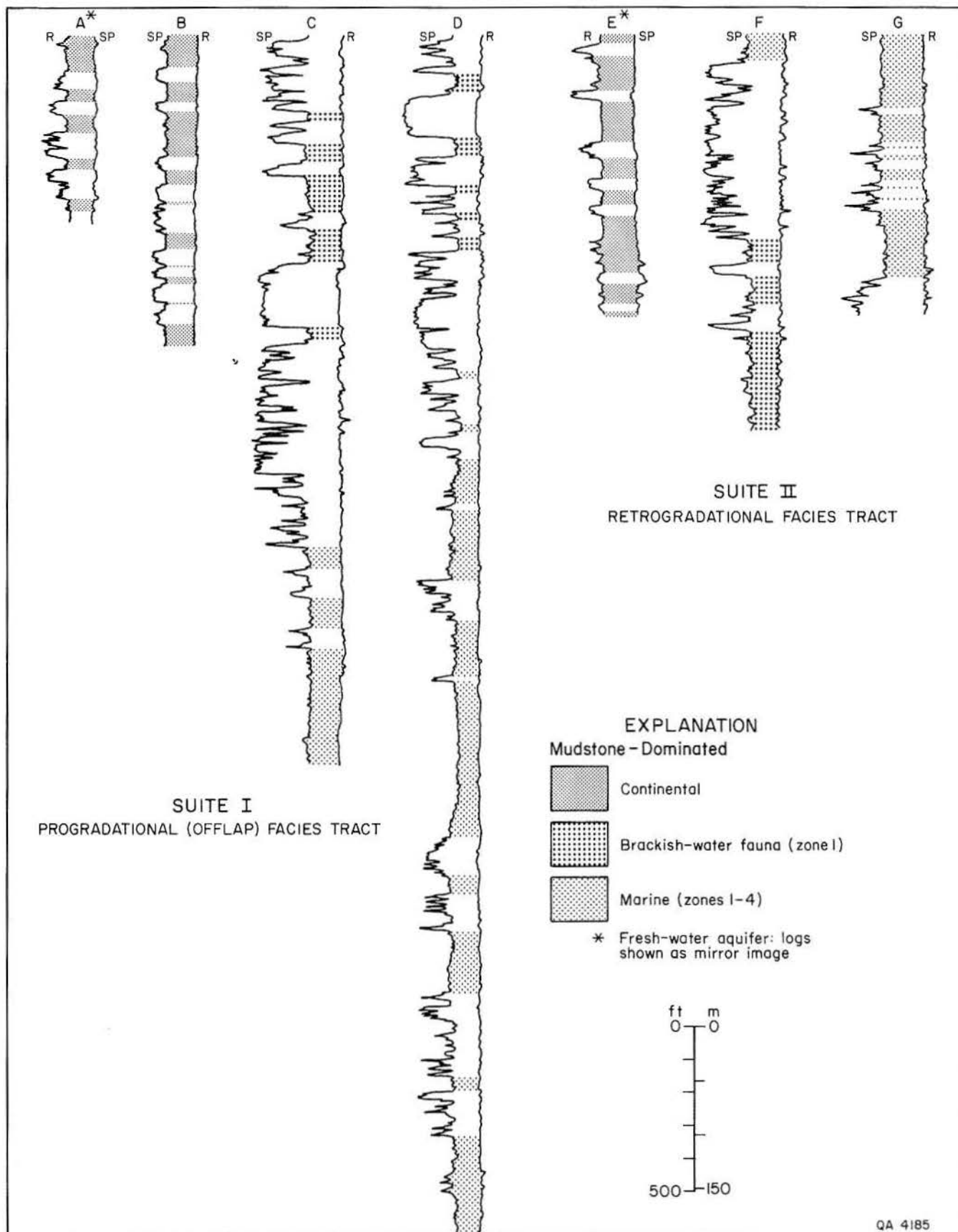


**Figure 5.** Electric log response of typical facies sequences within the depositional complex of a Gulf Coast Cenozoic episode. For well locations see figure 4.

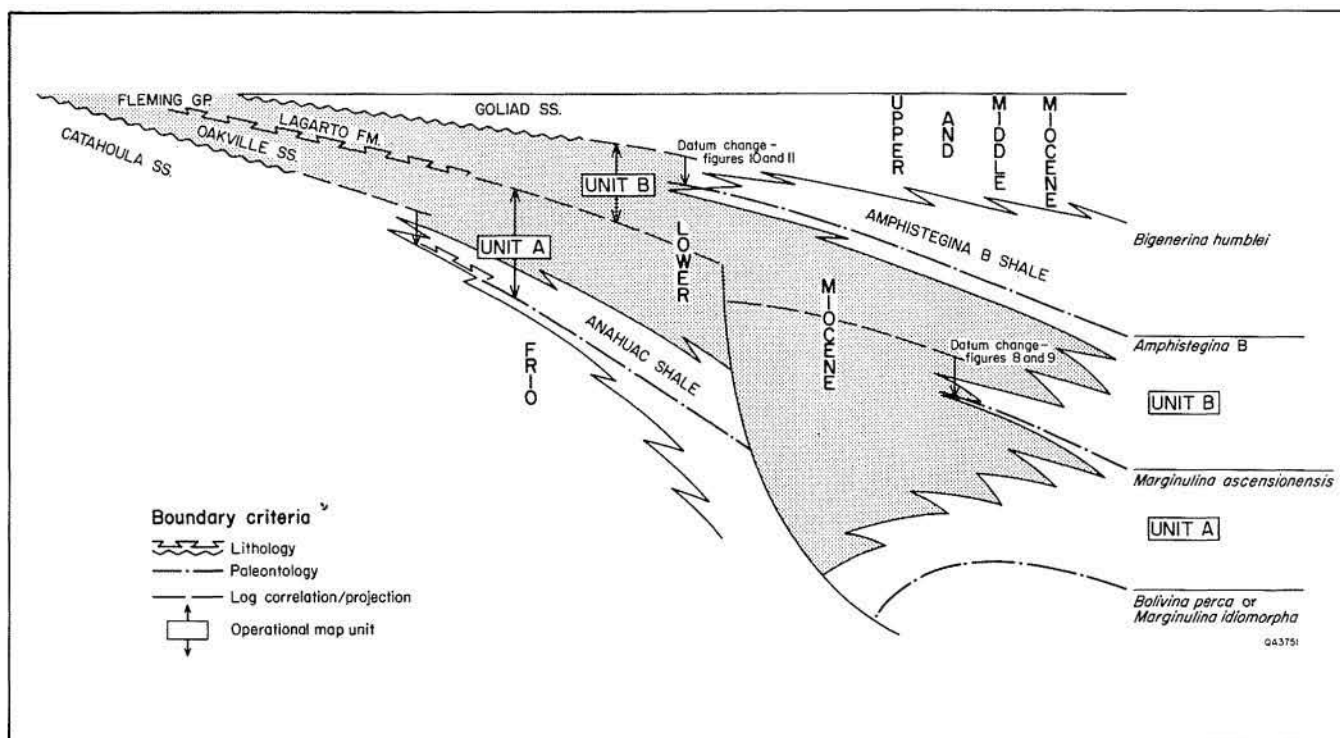


**Figure 6.** Schematic cross section of the lower Miocene depositional sequence, Texas Coastal Plain and shelf, showing the lithostratigraphic and biostratigraphic features used for correlation. The sequence is further subdivided into lower and upper operational map units A and B, which are informally named after the approximately equivalent Oakville and Lagarto Formations.

and others, 1985b), were correlated using the operational concepts of episode stratigraphy. Together, these sections provide a framework for correlation of infill control and subsequent facies mapping. Three reference dip sections, selected from the regional network to illustrate our correlations and subdivision of the lower Miocene sequence, are reproduced as plates 1 through 3. Section 1-1' (pl. 1) traverses a somewhat anomalous part of the study area in which the Lagarto operational unit significantly offlaps the underlying Oakville paleomargin. Sections 12-12' and 19-19' (pls. 2 and 3) are more typical examples of the contrasting progradational Oakville and retrogradational Lagarto facies sequences characteristic of the Texas Coastal Plain and shelf.

## Objectives

The objective of this analysis of the lower Miocene section is threefold:

(1) Delimit the principal depositional systems and their component genetic facies and paleogeographic elements.

(2) Synthesize the lower Miocene structural framework and establish its relationship to the depositional framework.

(3) Describe, within the geologic setting thus defined, the occurrence, distribution, and interpreted origin of hydrocarbon plays, and assess the potential for reserve additions or discovery of new plays.

The abundant well control of the coastal plain and in State waters provides an adequate data base for facies mapping and interpretation. Though drilling density on the Outer Continental Shelf (OCS) is comparatively sparse, depositional trends established updip may be confidently projected to downdip limits of control. In the absence of a systematic grid of seismic data, structural interpretations offshore are of necessity generalized. However, enough regional seismic data were made available by private companies and by the Minerals Management Service of the U.S. Department of the Interior to permit delineation of major structural features and interpretation of structural styles.

# STRUCTURAL FRAMEWORK

Structural styles exhibited by the lower Miocene section are typical of the Cenozoic fill of the northwest Gulf Basin. Principal features and provinces are shown in figure 7. Structures may be grouped into two assemblages: (1) reactivated structures inherited from the underlying depositional platform and (2) contemporaneous structures initiated or accelerated by lower Miocene continental margin progradation.

## Reactivated Structures

Reactivated structures include various features found landward of the Frio paleomargin. Principal examples include the Frio and Vicksburg fault zones, which were initiated by shelf-margin progradation and sedimentary loading during these earlier depositional cycles, and an extensive family of deep and shallow salt diapirs that extend throughout the Houston salt basin (fig. 7). The diapiric salt structures were largely mobilized by Eocene outbuilding of the continental slope onto thick, deeply buried Jurassic salt (Martin, 1978). Subsequent deposition and continental margin progradation embanked older structures during the Frio episode and reactivated diapiric growth and associated faulting. Frio structural trends were in turn reactivated by further burial by as much as several thousand feet of Miocene sand and mudstone. A few salt diapirs of the inner and middle shelf in the High Island and Galveston areas were likely mobilized by Miocene slope progradation. These comparatively young salt structures may display anomalously thickened lower Miocene sections within adjacent rim synclines.

Similarly, stresses resulting from renewed crustal subsidence and loading of the underlying Cenozoic continental platform reactivated many of the major down-to-the-basin growth-fault zones. Though displacement of the Neogene section is small compared with that typical of the deeply buried roots of the faults, it may exceed several hundreds of feet and have generated low-relief rollover anticlines or local dip reversals within lower Miocene deposits. Examples of such faults are prevalent in mid-dip segments of sections 12-12' and 19-19' (pls. 2 and 3).

## Contemporaneous Structures

As is typical of actively prograding, terrigenous divergent margins in general (Winker and Edwards, 1983) and of the Cenozoic Gulf Coast continental margin in particular (Jackson and Galloway, 1984), the downdip prism of lower Miocene deposits that built out beyond the underlying Frio continental platform initiated large-scale growth faulting and deep-seated sediment extrusion and uplift. Principal features include down-to-the-coast listric normal faults (growth faults), which exhibit large growth ratios and tremendous expansion of section on down-dropped sides, and strike-parallel shale ridges, which display both contemporaneous uplift and sediment damming as well as diapiric intrusion and late-stage faulting. Two styles of growth faulting are apparent. Closely spaced, laterally discontinuous fault zones typify the lower Miocene wedge beneath Mustang Island and areas to the south and in the Galveston and High Island areas, where some salt diapirism also complicated the stress field. In the Matagorda and Brazos areas, a single, laterally continuous belt of faults parallels the initial position of offlap of the lower Miocene episode beyond the Frio paleomargin (fig. 7; wells MJF-6 through MJF-11, section 12-12', pl. 2). Shale ridges and associated counter-regional (up-to-the-basin) faults are also prominent in the middle Texas shelf. This segment of the Miocene continental platform is bounded basinward by the Brazos-Matagorda ridge, which was the locus of a similarly continuous, highly listric upper Miocene fault complex.

The depositional and structural processes initiating and driving growth faulting and associated shale ridge emplacement were discussed by Bruce (1973), Dailly (1976), and Crans and others (1980). Discussion of the mechanics of growth-fault and shale ridge formation is beyond the scope of this report; however, as Jackson and Galloway (1984) pointed out, several proposed mechanisms are probably involved. Nevertheless, the apparent association of fault geometry with regional facies trends, discussed in the next section, suggests a genetic relationship between deposition and structural style.



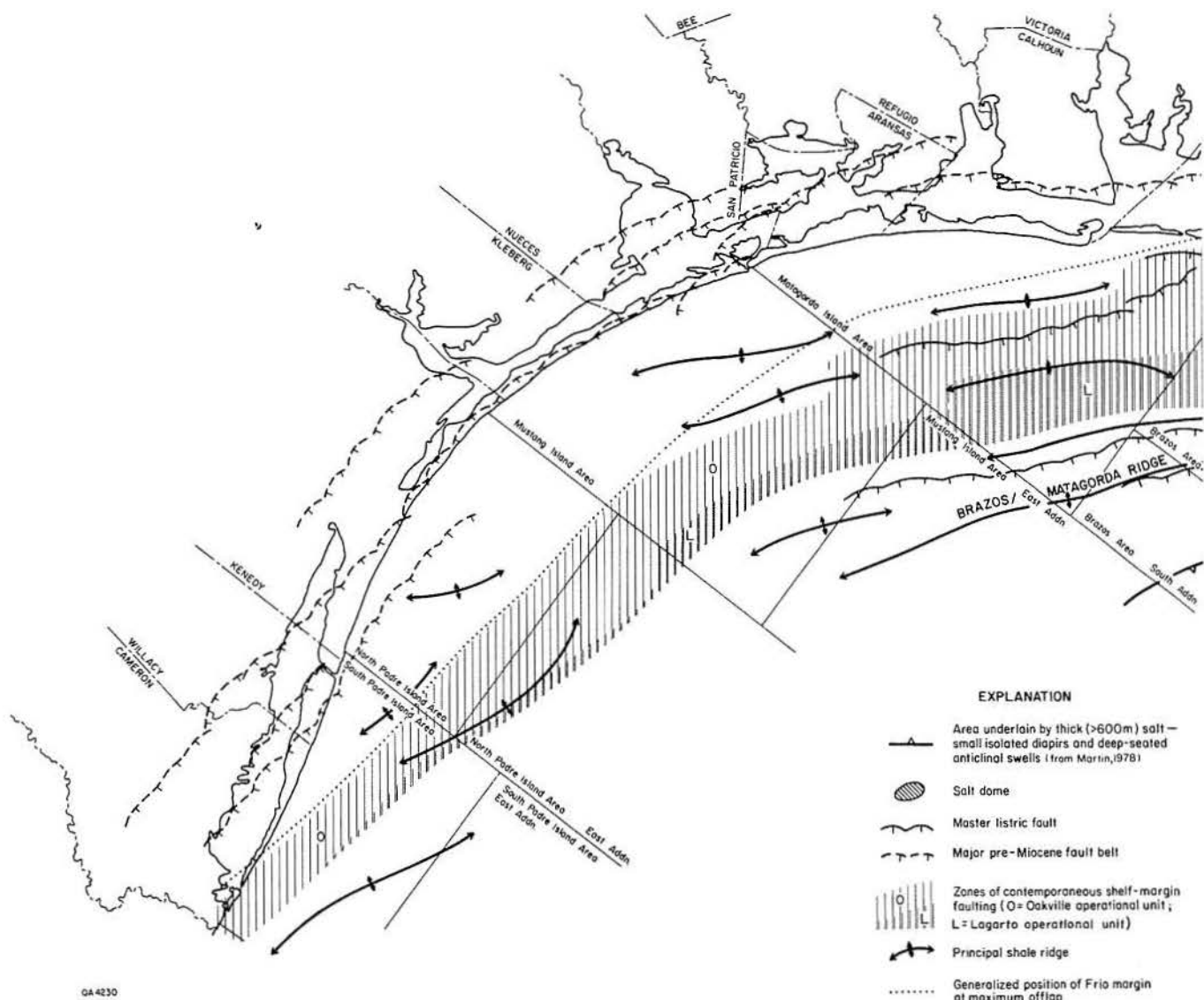
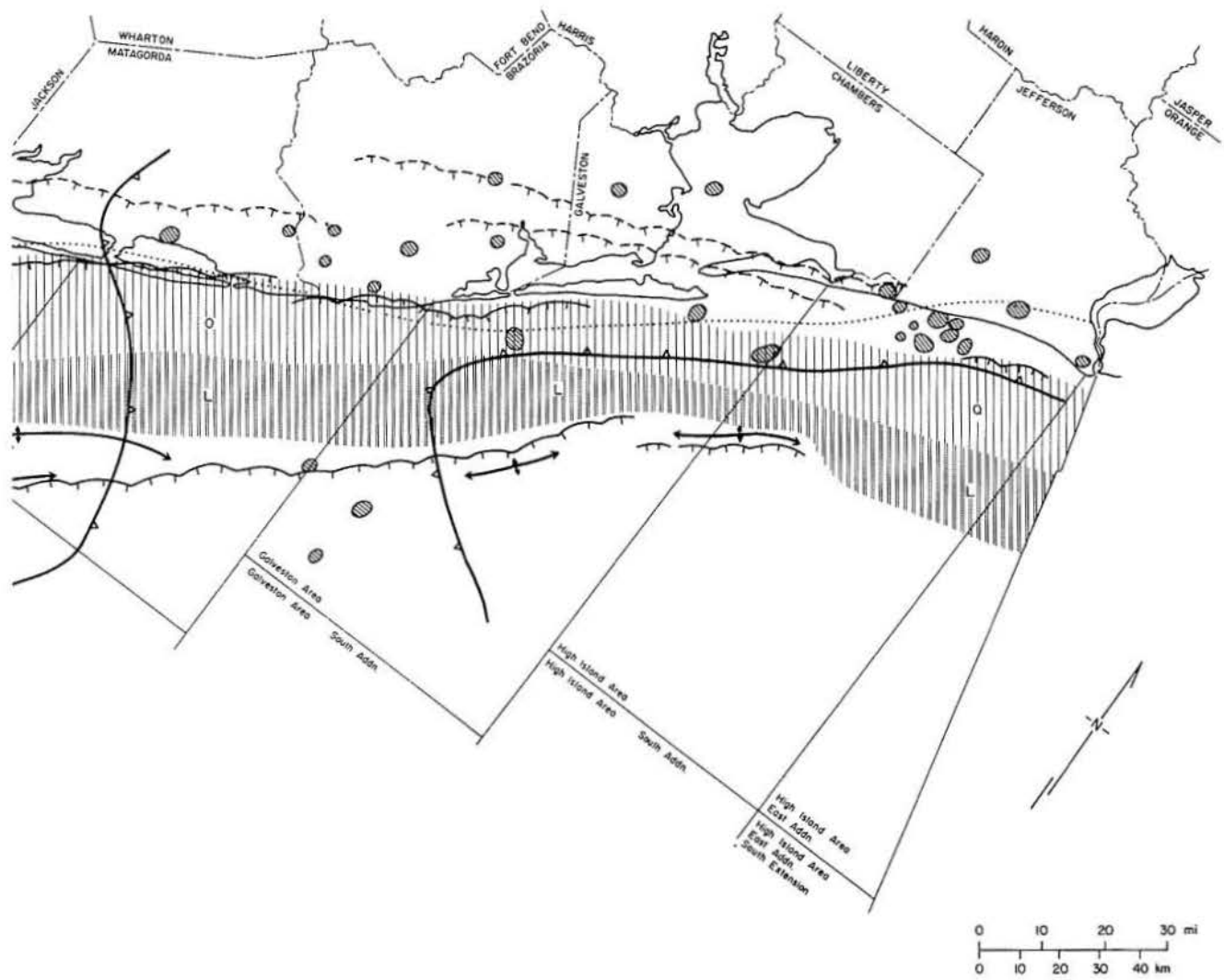


**Figure 7.** Structural framework of the lower Miocene sequence. Major features that affect the Fleming section include inherited fault zones and diapir swarms, contemporaneous shelf-margin extensional faults and shale ridges, and younger Miocene extensional faults. Compiled in part from numerous published and unpublished sources.



# LOWER MIOCENE DEPOSITIONAL FRAMEWORK

The following overview of lower Miocene deposition synthesizes and elaborates many of the ideas and interpretations presented by Doyle (1979), Spradlin (1980), Solis (1981), Galloway and others (1982a), DuBar (1983), and Morton and others (1985a) in discussions of specific areas of the Texas Coastal Plain or shelf. Rainwater (1964) provided the most complete overview of Miocene sedimentation in the northern Gulf Coast and noted the presence of the major delta system in Louisiana, a smaller deltaic complex centered on the Rio Grande Embayment, and a mainly interdeltic shoreline between. This generalized paleogeography is substantiated by the detailed mapping and interpretation presented here.

## Sources of Data

Principal data sources include several thousand geophysical logs of wells drilled through or into the lower Miocene section. These wells were correlated into 24 Gulf Coast regional cross sections (Dodge and Posey, 1981) and their offshore extensions (Morton and others, 1985b). Correlation sections are on open file at the Bureau of Economic Geology.

The utility of electric log pattern interpretation and mapping in Gulf Coast Cenozoic systems was demonstrated by Fisher and others (1969) and more recently was systematically applied by Galloway and others (1982a, 1982b) to the Frio depositional episode. Genetic facies interpretations, based on analysis of electric log patterns, of the lower Miocene interval (Morton and others, 1985a) are substantiated in this study, further indicating the utility of this technique for subsurface facies analysis. Because continuous lower Miocene core is sparse, log pattern interpretation was a major tool for determination of lithology and vertical sequence.

Quantitative facies maps form the foundation of the facies interpretation. Net-sandstone and sandstone-percent maps were prepared for both operational units and are presented as figures 8 through 11. Our method of map compilation requires some explanation. Onshore, the maps are largely composites of

earlier mapping. Updip, published and unpublished maps of Oakville and Lagarto lithofacies by Galloway, supplemented by East Texas maps of Spradlin (1980), detail shallow subsurface facies patterns. Original data for these maps were compiled from more than 1,000 shallow wells; data points are not shown on the highly reduced versions included here. DuBar (1983) mapped mid-dip areas, and, with some modification necessitated by revised correlation and new well control, his maps are incorporated in the regional mapping. Well spacing used was relatively uniform, averaging about 10 to 15 mi (16 to 25 km) between control points. The lower coastal plain and continental shelf areas were mapped using all available deep well control. Because well distribution is more erratic offshore, locations of data points in this area are shown on each map. In addition, large-scale versions of each map are included as plates 4 through 7.

The composite nature of the regional maps necessitates a word of caution. The original maps from which they were compiled reflect different densities of well control, selections of operational correlation points, and criteria for definition of sand on the geophysical logs used. Nonetheless, we feel that the composite maps, though locally incorporating some artistic license in the merging of contours, do correctly reflect primary facies trends and typical lithologic compositions.

Lower coastal plain and shelf areas reflect a carefully tied correlation network and a systematic sand-counting procedure. However, two additional points concerning the downdip mapping should be made. First, the major datum change shown on each map reflects a correlation adjustment that must be made in going from the nonmarine part of the lower Miocene depositional complex to that bounded by marine shales. Absolute values may change substantially across this datum change, but overall contour pattern is typically little affected. Second, few wells penetrate the complete lower Miocene section within its expansion zone. To extend facies mapping into this critical area, an isopach map of the total Oakville operational unit was constructed

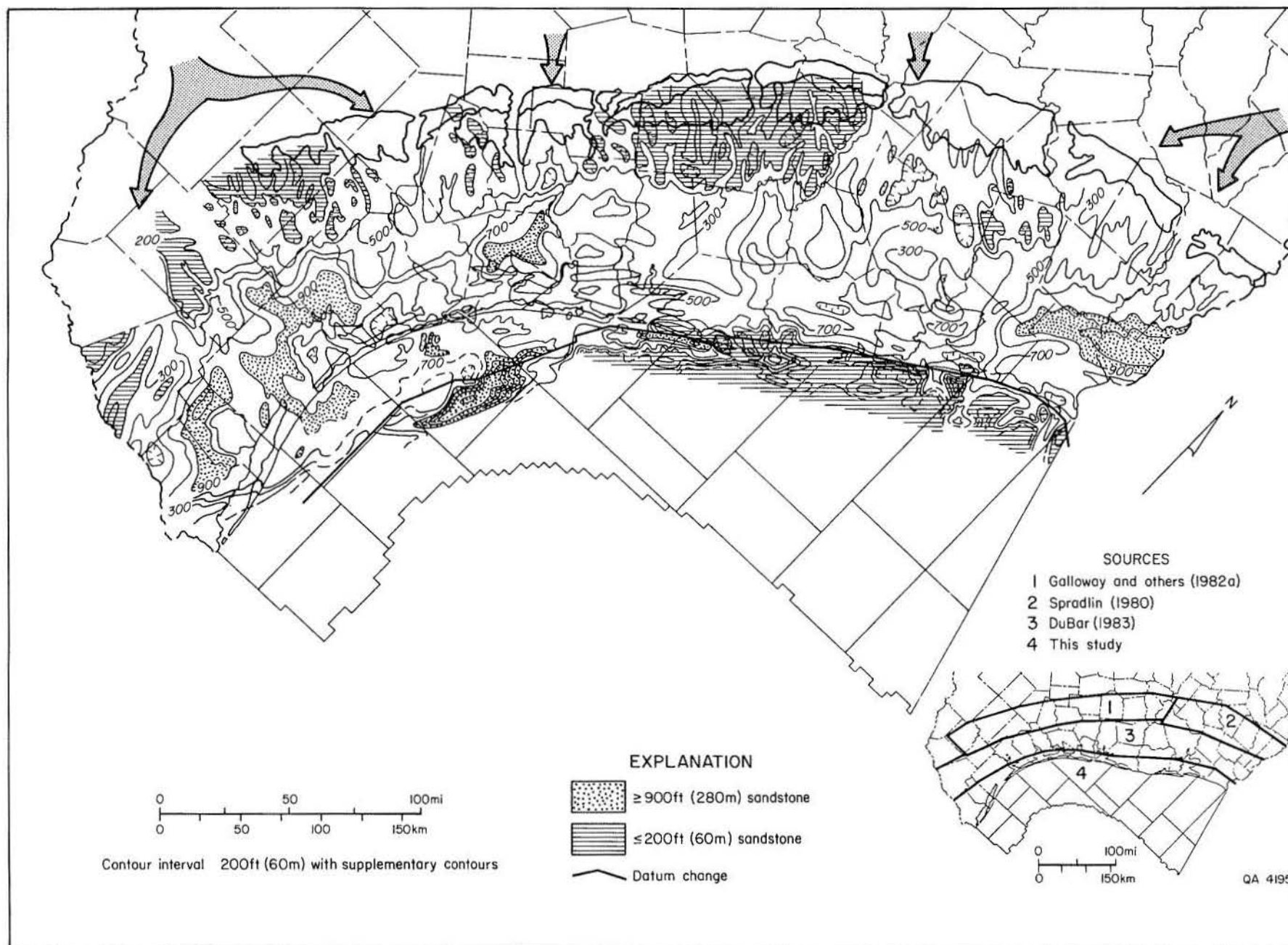


**Figure 8.** Net-sandstone isopach map of the Oakville (Anahuac shale to *Marginulina a.*) operational unit.



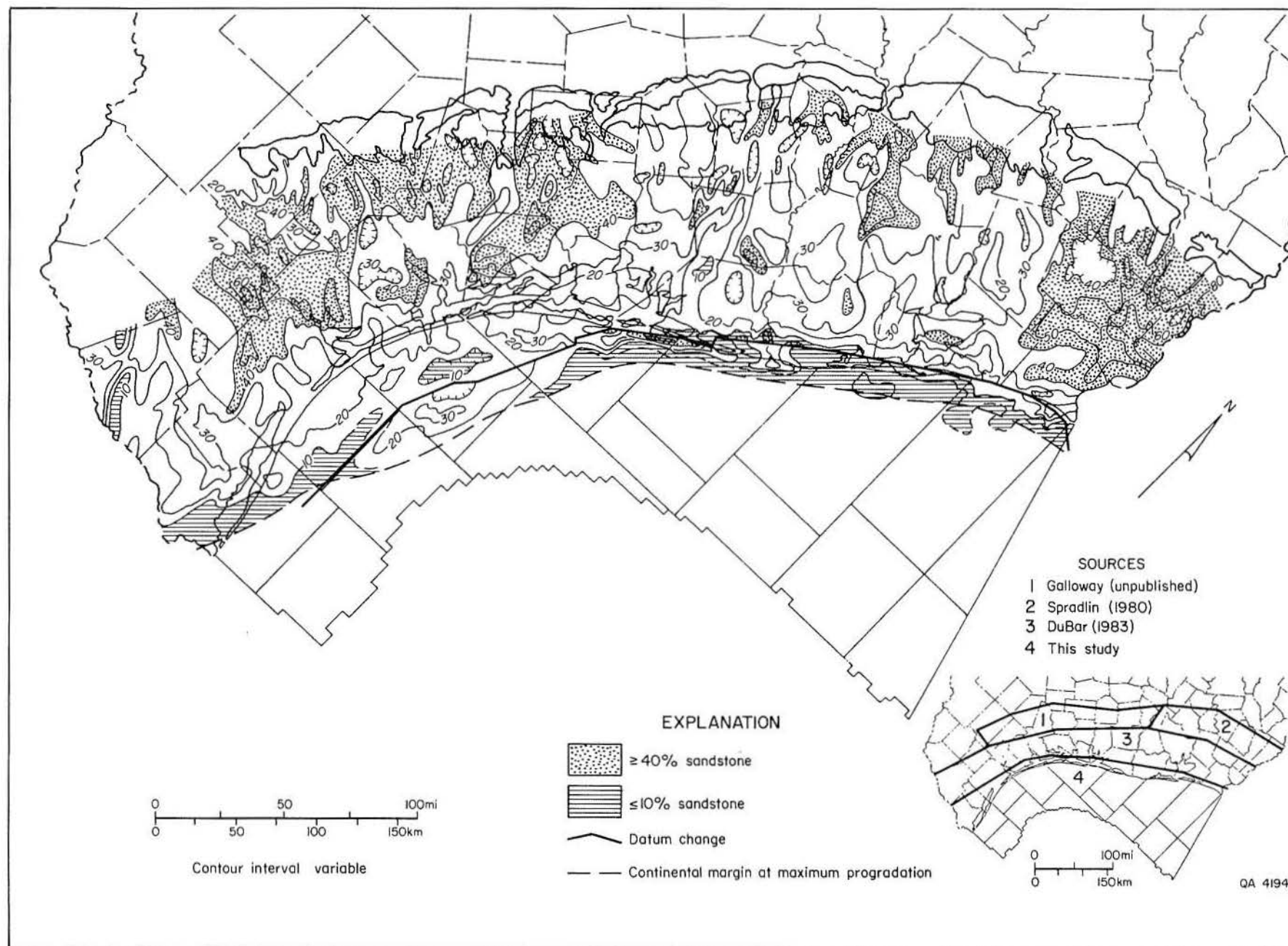


**Figure 9.** Percent-sandstone map of the Oakville (Anahuac shale to *Marginulina a.*) operational unit.

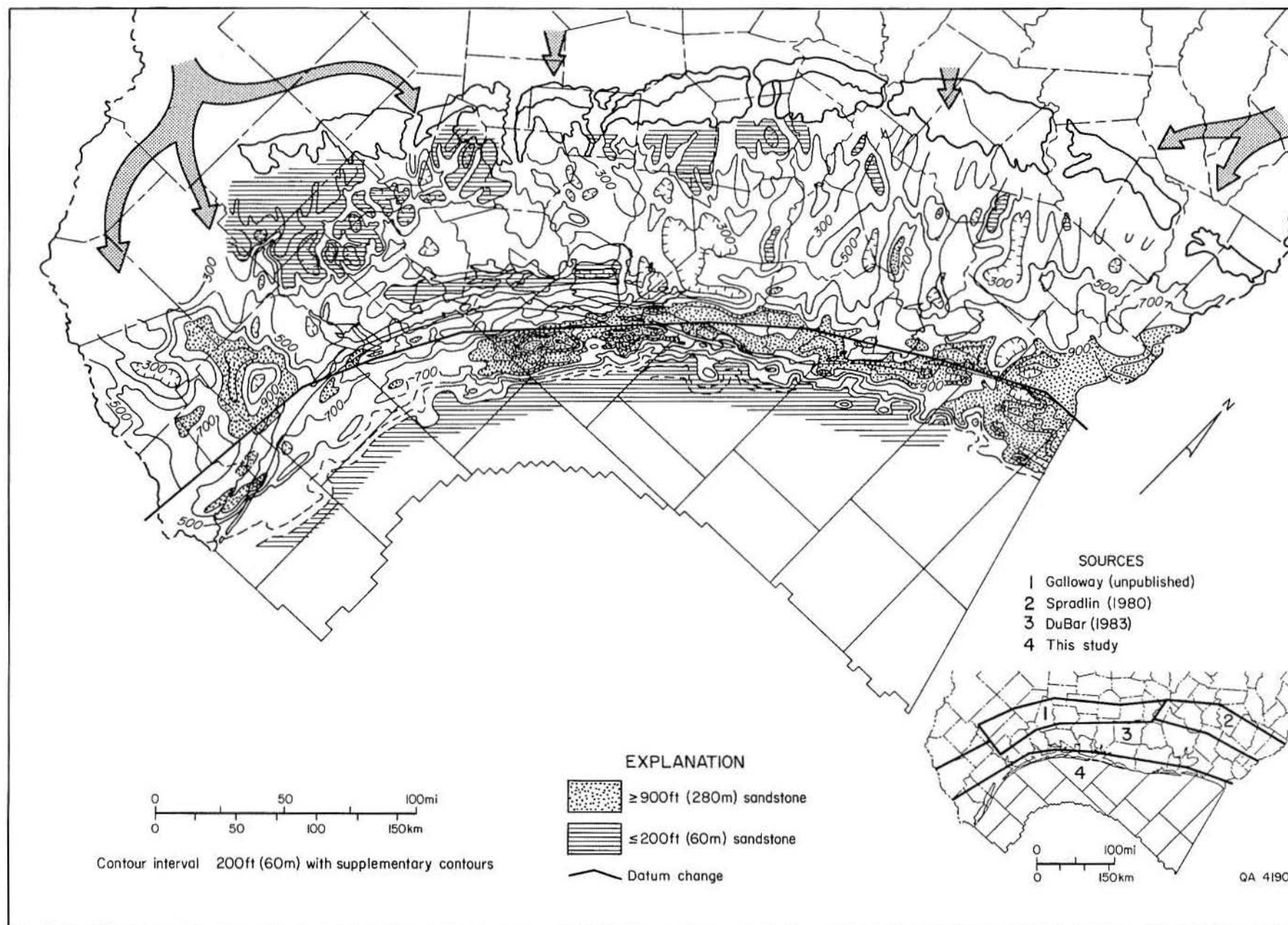


**Figure 10.** Net-sandstone isopach map of the Lagarto (*Marginulina a.* to *Amphistegina B* shale) operational unit.

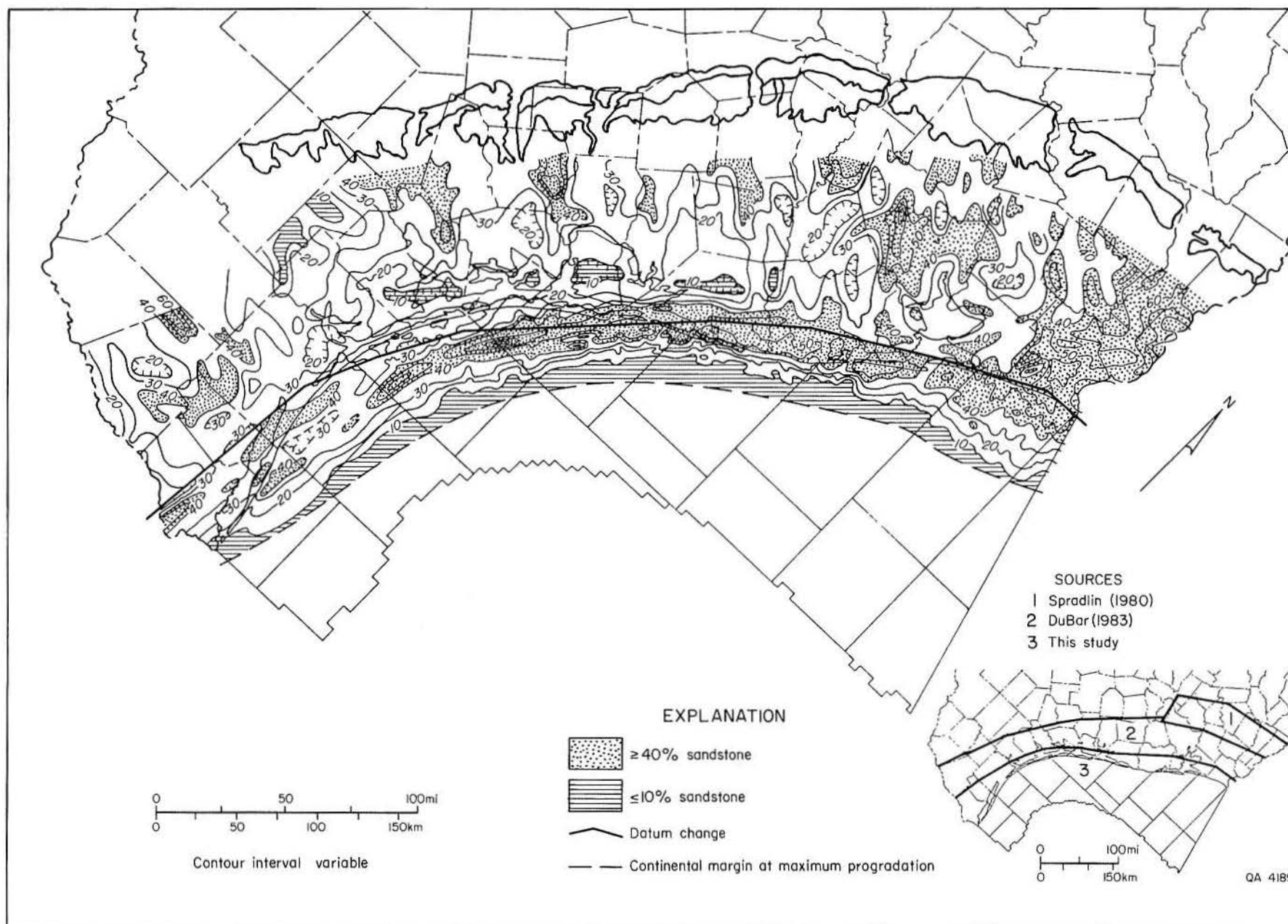


**Figure 11.** Percent-sandstone map of the Lagarto (*Marginulina a.* to *Amphistegina B* shale) operational unit.

using the deepest wells. In each well that penetrated more than 50 percent of the inferred total unit thickness, net- and percent-sandstone values were calculated using assumptions that sand content of the undrilled section equaled 0, 50, and 100 percent of that in the penetrated section. Finally, the regional dip sections were used to choose the most likely assumption about sandstone content, and the selected value was plotted. The validity of the resultant maps is supported by the somewhat surprising observation that, in this sand-poor section, all three assumptions about sand content commonly resulted in a relatively small range of calculated values for any individual well.

In addition to lithofacies information derived from geophysical logs, paleontologic summaries of more than 60 wells aided definition of marine sections and provided paleoecologic information. Marine paleobathymetric zones are commonly classified as transitional (brackish), inner shelf (ca. 0 to 70 ft, or 0 to 20 m), middle shelf (ca. 70 to 300 ft, or 20 to 100 m), outer shelf (ca. 300 to 600 ft, or 100 to 200 m), upper slope (ca. 600 to 1,500 ft, or 200 to 500 m), and lower slope (ca. 1,500 to 6,000 ft, or 500 to 2,000 m). Data are grouped into inner shelf, outer shelf/slope transition, and slope environmental assemblages and plotted on figure 12. Three broad paleoecologic belts are delineated by the generalized paleobathymetric contours, which are drawn to reflect the shallowest water depths commonly recorded through much of the Oakville and Lagarto intervals. Transitional through upper slope zones correspond to the areas of lesser Miocene sandstone development (compare figure 12 with figures 8 through 11). Deeply buried, sand-poor lower Miocene sections contain upper to lower slope faunal assemblages. Although paleoenvironmental interpretation is subject to differences in zone definition and limits of sample recovery and quality, the broad paleobathymetric zones defined are quite homogeneous, and they parallel facies trends outlined by isolith mapping.

Systematic description of outcrops and shallow cores incorporated in previous uranium-related studies provided useful information for interpreting the updip section.

Few cores of mid- and downdip Miocene wells were available, however. Analysis of systematically assembled cores would aid in further detailed description of depositional facies and is a prerequisite for determining the effect of diagenesis on reservoir quality.

## Lower Miocene Depositional Systems

Figure 13 shows the interpreted distribution of lower Miocene depositional systems and major component facies assemblages. The quantitative facies maps clearly indicate the presence of three major depositional regimes characterized by differing trends and abundance of framework sandstones.

In South Texas, several laterally adjacent, dip-oriented belts of sand grade basinward into mixed dip and strike trends. This major fluvial and deltaic complex corresponds to a broad, poorly defined axis of the Rio Grande Embayment. A similar fluvial/deltaic complex extends downdip across the easternmost part of the Texas Coastal Plain and shelf, where mixed dip and strike contour trends are apparent. This feature seems to be only the western margin of a larger system centered in Louisiana, the location of the major Miocene depocenter. Between the two fluvial/deltaic complexes is a strongly strike-aligned, sandy microtidal shore-zone system separated by a sand-poor belt from a coastal plain traversed by numerous minor fluvial axes.

In the following sections, each of six principal depositional systems recognized will be discussed in detail.

### Santa Cruz Fluvial System

A major lower Miocene fluvial system extends from the partly covered outcrop across the shallow subsurface of the South Texas Coastal Plain (fig. 13). This coarse-grained, locally conglomeratic fluvial sequence has been studied in considerable detail because of its uranium deposits (Galloway and others, 1982a).

Detailed facies mapping revealed two principal entry points, or fluvial axes, for this system. The southerly Hebbronville axis is known only in the subsurface, extending



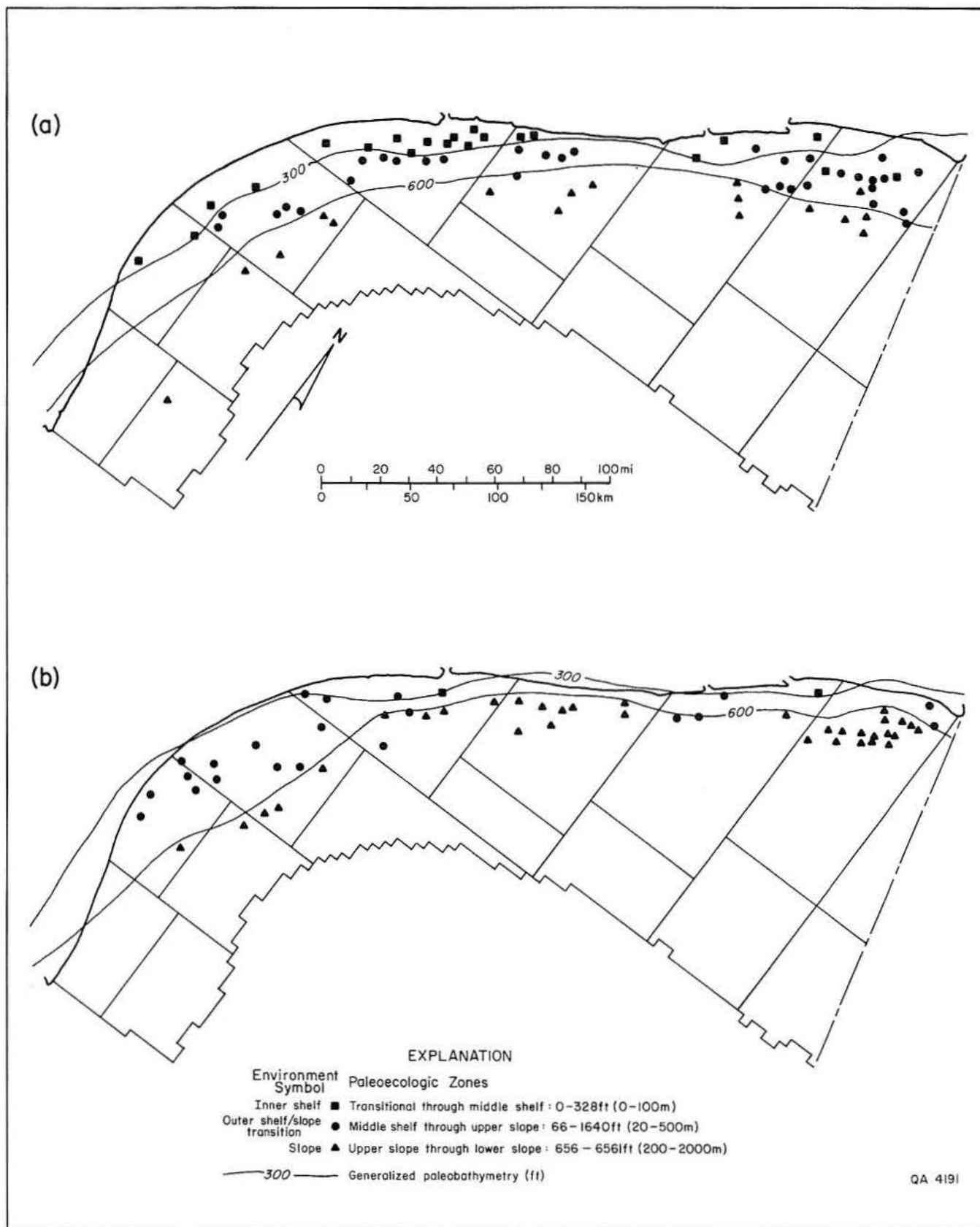


**Figure 12.** Generalized paleobathymetry of (a) Oakville and (b) Lagarto map interval mudstones. Paleoecologic determinations are based on benthonic foraminiferal assemblages. Where more than one depth zone was identified within the interval, shallowest zones are emphasized.

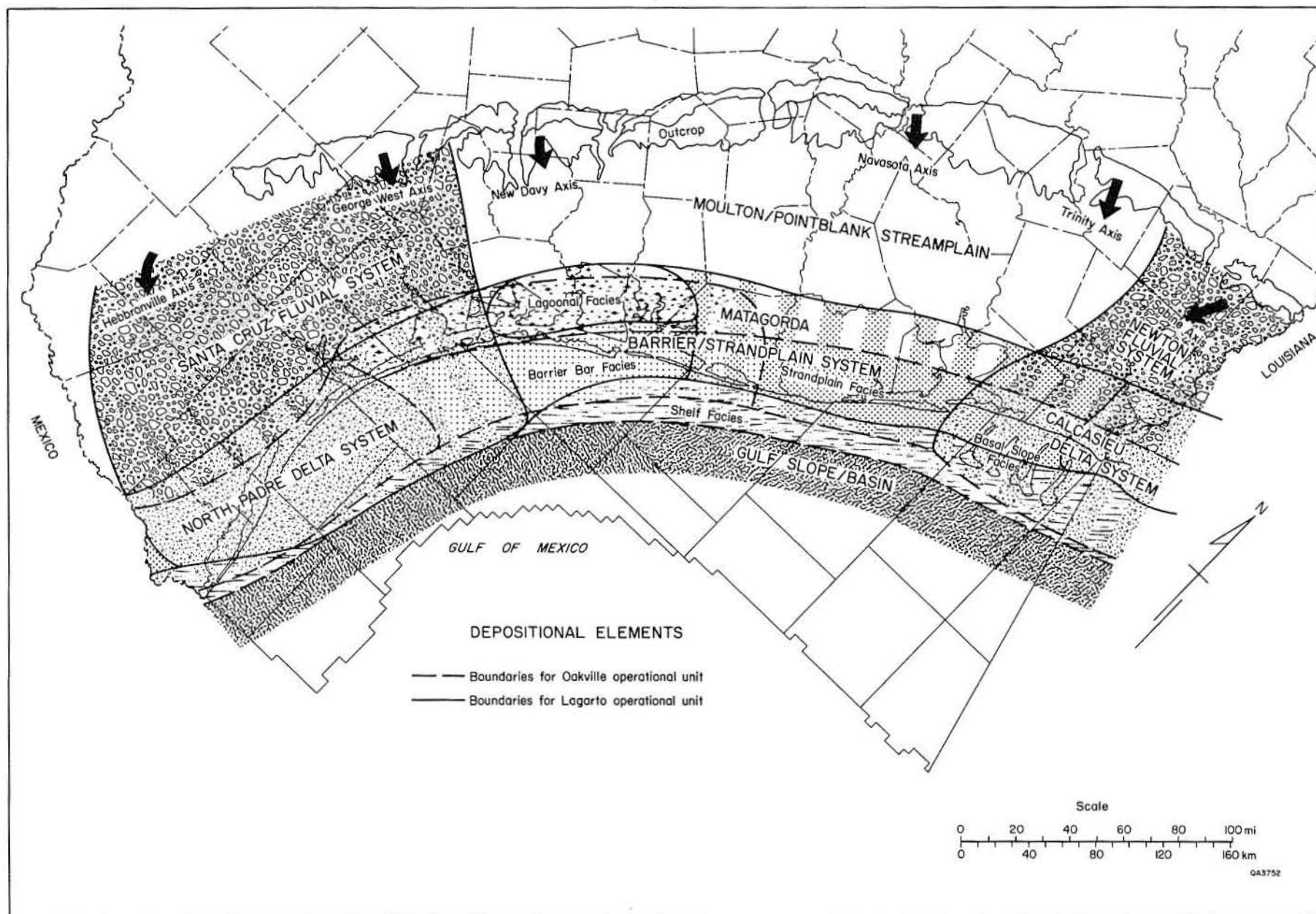


**Figure 13.** Lower Miocene depositional systems and their component elements.

basinward from the Goliad-covered subcrop in Jim Hogg County. The George West axis, centered in Live Oak County, has been dissected by uranium mining, and here paleocurrent data and lithofacies maps of the shallow subsurface section indicate easterly channel trends near the outcrop. The apparent landward convergence of projections of the two fluvial axes, combined with the occurrence of a pebble suite indicative of a Trans-Pecos source area in the George West channel sand bodies, led Galloway and others (1982a) to conclude that the axes are two stable entry points of the same major drainage system into the Gulf Coast Basin. Both axes appear to have been reoccupied numerous times; however, the Hebbronville axis is the more prominent of the two on the Lagarto unit maps.

The Santa Cruz fluvial system is sand rich. In the Oakville unit, sand percentage commonly exceeds 40 percent (fig. 9). Decreased proportion of sandstone in the Lagarto reflects increased aggradation and preservation of floodplain facies. Composition, sandiness, and internal structures all indicate that the system was characterized by low sinuosity, typically braided bed-load channels (Galloway and others, 1982a). Typical log response for sandy, aggradational sequences of Santa Cruz fluvial deposits is shown by wells DP-16 through DP-22 on section 19-19' (pl. 3).

### North Padre Delta System

The Santa Cruz bed-load fluvial system merges basinward into delta-plain deposits of a large though diffuse deltaic complex, the North Padre delta system. The landward margin of the delta system is placed (fig. 13) at the updip limit of the bounding marine shale wedges. Deposition of basal Oakville prodelta mud and delta-front sand over Anahuac marine mud initiated deltaic progradation. Down-dip, the North Padre delta complex extends far offshore across the Mustang and North Padre Island areas. Thus, the system is generally coincident in areal distribution with the underlying Frio Norias delta system. Only the distal margin of the North Padre delta system prograded beyond this underlying deltaic continental platform to form a narrow lower Miocene

expansion zone (shown by wells MJF-8 and MJF-9, section 19-19', pl. 3).

The southern margin of the delta system probably closely parallels the present course of the Rio Grande. Northward, the system merges into interdeltic coastal deposits.

Sand-rich, strongly strike-parallel delta-margin facies trends typify the North Padre delta system. Log patterns are blocky (wells MJF-4 through MJF-7, section 19-19', pl. 3), as is typical of aggradational coastal-barrier sands that front high-destructive, wave-dominated deltas (Fisher and others, 1969). Vertical sequence and strong strike alignment of the framework sands show the North Padre delta system to have been wave dominated. The facies tract consists of (1) delta-plain channel and overbank deposits, (2) sand-rich coastal-barrier and beach-ridge units reworked and deposited along the delta front, and (3) prodelta, shelf, and upper slope muds containing thin, discontinuous distal delta-front slump, turbidite, and storm beds as well as outer-shelf to slope faunas.

The North Padre system probably grew in a manner much like that of the late Quaternary Colorado/Brazos deltaic complex. As pointed out by Winker (1979), these smaller deltaic systems of the Gulf margin form broad convex depositional headlands in which active sediment input and progradation are limited to a very small area at any one time. Along most of the headland, marine reworking, sediment redistribution, and coastal aggradation dominate. Such headlands may be as wide as 100 mi (160 km), comparable to the dimensions of the North Padre delta system. This pattern of slow delta growth accompanied by large-scale marine redistribution of sediments deposited at active channel mouths explains an apparent anomaly visible on the facies maps: thickest sandstone sequences and greatest continental margin offlap occur in the interdeltic reentrant to the northeast of the delta system and not within the perimeter of the delta system (figs. 8 and 10). Several modern marine-dominated deltas, including the Orinoco delta of Venezuela and the Copper River delta of Alaska, display similar lateral offset of their depocenters from the active delta front (van Andel, 1967; Galloway, 1976). Lower Miocene

deltaic sedimentation reestablished the Frio deltaic platform in the face of ongoing compactional and isostatic subsidence (of as much as 6,000 ft [1,800 m]). However, reworking of both mud and sand northward alongshore left little additional sediment for progradation of a new continental platform. Thus, lower Miocene continental margin progradation formed a narrow belt no more than 15 to 20 mi (25 to 35 km) wide across the Mustang, North Padre, and South Padre Island areas. In contrast, the Frio prograded the continental platform as much as 70 mi (115 km) seaward within a comparable period (7 Ma) (Galloway and others, 1982b).

During the retrogradational part of the lower Miocene episode, deltaic progradation was further restricted, strike redistribution of delta-margin sands by wave action was even more pronounced (fig. 11), and the area that can be considered to be even minimally deltaic retreated southward (fig. 13).

### Moulton/Point Blank Streamplain

The Moulton streamplain, a belt of inner coastal plain sediments containing the deposits of numerous small local streams (first named by Galloway and others, 1982a), is extended in this report to the northeast to include the Navasota and Point Blank drainage systems defined by Spradlin (1980). The system thus constitutes a comparatively thin, updip apron of lower Miocene sediment stretching from Bee through Polk Counties (fig. 13).

The New Davy, Navasota, and Trinity fluvial axes are prominent on lithofacies maps of both operational units. These axes contain the typical Oakville calc lithic sandstones of the middle Texas Coastal Plain outcrop belt and derived their sediment load from Cretaceous rocks exposed around the rim of the basin and in the Edwards Plateau.

Facies include generally thin channel-fill units of ephemeral to sinuous, perennial streams encased within commonly calcareous floodplain mudstones. Flashy flow resulted in widespread dispersal of sheet- and crevasse-splay aprons about the small channels (Galloway and others, 1982a). Typical lithologic sequences and their log response are

illustrated by wells DP-8 and DP-9 on section 12-12' (pl. 2).

### Matagorda Barrier/ Strandplain System

The Moulton/Point Blank streamplain is bounded basinward by thick coast-parallel mud- and sand-rich belts of a lower Miocene interdeltic shore-zone depositional complex. This shore-zone system corresponds in part to the informally designated subsurface "Oakville bar," a massive, strike-trending sandstone unit penetrated by wells DP-13 and MJF-2 through MJF-4 on section 12-12' (pl. 2). It is here named the Matagorda barrier/strandplain system because the system is well developed beneath both Matagorda County and the Matagorda Island OCS area. As shown on figure 13, the barrier/strandplain system is the principal depositional element of the Fleming depositional sequence in Texas. It extends from a transitional boundary with contemporaneous streamplain deposits, which lies approximately 40 mi (65 km) inland of the present shoreline, down to and across the Miocene expansion zone (fig. 13). Lateral boundaries were transitional and shifted greatly through time. Generally, the entire system expanded southward about 40 mi (65 km) during deposition of the Lagarto unit.

A prominent strike-parallel belt of sandstone forms the core of the shore-zone system. The greatest thicknesses of sandstone within the lower Miocene depositional episode are found where this belt overlaps the expansion zone in the Matagorda and Mustang Island areas (figs. 8 and 10). For example, within the Lagarto unit alone more than 2,000 ft (600 m) of sandstone is stacked in the downthrown block of a major growth fault in the Matagorda Island area (fig. 10). Sandstone percentage is comparably high along the trend, commonly exceeding 40 percent and even as much as 60 percent of several thousand feet of section. The sand-rich trend is further emphasized in that it is bounded both updip and downdip by mud-rich belts containing less than 20 percent sandstone. Thus, the Matagorda barrier system displays a consistent facies tract (pl. 2) characterized by (1) a



basinward mudstone sequence containing a diverse marine fauna indicative of outer-shelf to upper slope water depths; (2) a transitional zone of thin distal shoreface and inner-shelf sandstone and siltstone interbedded with shelf mudstone; (3) a narrow (10 to 15 mi [15 to 25 km]) belt of massive, vertically and laterally amalgamated, aggradational and bounding progradational sand bodies exhibiting strong strike alignment and separated by inner-shelf and transitional mudstones; and (4) a landward zone of massive mudstone containing scattered, generally thin sandstone units, which display mixed blocky and progradational log patterns.

The shore-zone complex is interpreted to be a mix of microtidal barrier-island and sand-rich strandplain deposits on the basis of (1) the dominance of narrow, strike-parallel sand bodies, (2) the inferential oceanography of the Neogene Gulf of Mexico (a Mediterranean-type seaway, generally isolated from the Atlantic Ocean and its tidal system), and (3) the close similarity of the lower Miocene facies tract to that of the better known Frio Greta/Carancahua barrier/strandplain complex (Galloway and others, 1982b; Galloway, 1984; Tyler, 1984).

The thick updip mudstone sequences that lack a marine fauna and contain few sand bodies are strongly indicative of large impounded water bodies—bays and lagoons. Distribution of this facies assemblage delimits the corresponding extent of well-developed barrier bars along the interdeltic shoreline. Here, the thick sandstone belt consists of barrier core, inlet fill, shoreface, and various back-barrier facies. Where streams filled the bays and lagoons, channel deposits merge directly with the shore-zone sands, providing multiple points of additional sediment input to the shoreface. Such sandy strandplain deposits characterize the Matagorda system along the southwestern margin of the northern fluvial/delta complex (fig. 13) and are more abundant in the Oakville operational unit. The sandstone belt is a composite of beach-ridge, shoreface, and local channel and channel-mouth bar deposits.

The Matagorda barrier/strandplain system displays an aggradational regional depositional architecture. As shown in figure 13, Lagarto facies belts are essentially stacked

upon the sandy foundation constructed by Oakville progradation to and beyond the foundered Frio paleomargin. Structurally, the broad, muddy lower Miocene shelf was deposited behind, and buttressed by, prominent shale ridges. Linear loading by deposition of the tremendous sequences of shore-zone sands may well have accentuated growth of comparably elongate shale ridges such as the Brazos/Matagorda ridge (fig. 7).

## Newton Fluvial System

The northeastern margin of the map area contains thick, vertically and laterally amalgamated sand bodies that exhibit blocky or upward-fining log patterns and dip-oriented contour trends. Discontinuous mudstone lenses are interspersed through the section (wells DP-9 through DP-11, and the upper parts of wells DP-12 through DP-14, section 1-1', pl. 1). Downdip, the sand belts merge into a diffuse sand-rich area centered in Orange and Jefferson Counties (figs. 9 and 11). Outcrop features (Spradlin, 1980), trend, and paleogeographic setting all indicate a fluvial origin for these deposits. The magnitude of sand-body dimensions and the well-known presence of the major lower Miocene fluvial/deltaic depocenter in Louisiana (Rainwater, 1964) support the recognition of this sequence as a separate depositional system, or more correctly as the westernmost fringe of the Louisiana paleo-Mississippi system. The poorly defined Sabine fluvial axis (fig. 13), which is centered in Jasper County, may have been a tributary of the larger Louisiana system, or may represent the westernmost entry point for this continental-scale river into the Gulf Basin. Mapping of the lower Miocene of Louisiana will be required to resolve this ambiguity.

Sands of the Newton fluvial system are fine to medium grained. Outcrop features and detailed sand-body geometry indicate meandering channel patterns (Spradlin, 1980). Meanderbelt and crevasse splay deposits constitute the sandstone facies of this mixed-load fluvial system. Basinward, the system may become increasingly suspended-load dominated.

The basinward limit of fluvial deposition shifted landward in response to Anahuac,

*Marginulina* a., and *Amphistegina* B transgressions (pl. 1). The presence of oysters in the Burkeville fauna (Newton County) indicates that marine influence extended far inland in what must have been a very low-relief segment of the coastal plain. Superposition of strandline and fluvial facies in mid-dip areas, as well as development of broad but probably fine-grained meanderbelts on the lower coastal plain, produced the diffuse sandy facies belt along the downdip part of the system.

### Calcasieu Delta System

Like the Newton fluvial system, only a small segment of the principal lower Miocene deltaic depocenter, here named the Calcasieu delta system, extends beneath the Texas Coastal Plain and adjacent offshore area (fig. 13). The Calcasieu delta includes the *Planulina* trend deltas described by Caughey (1981). Mapped lobe complexes of the Louisiana Miocene deltas (Curtis, 1970) display sand isolith patterns typical of digitate fluvial-dominated to wave-dominated deltas.

In the map area, the Calcasieu delta system is best developed in the Lagarto unit. Progradation during later stages of the Fleming depositional episode constructed a prominent seaward bulge in the continental margin (fig. 10). The offlap sequence is punctuated by numerous closely spaced growth faults, which define the Miocene expansion zone in the High Island and High Island East areas (pl. 1). All but this downdip margin of the delta system overlies the Houston salt dome province; delta deposits are pierced or uplifted by numerous domes. Irregularly lobate sand distribution patterns (fig. 11) define lobe complexes that grade landward into dip-oriented fluvial facies trends and laterally into strike-parallel strandplain sand bodies of the Matagorda shore-zone system. The delta system contains two principal facies assemblages: (1) interbedded thick prodelta mudstones and expanded sandy progradational sequences deposited along the distal margin (wells MJF-11 through MJF-17, section 1-1', pl. 1) and (2) stacked delta-front, coastal-barrier, and delta-destructive shoreline sandstones that compose the main body of the delta complex. The wave-reworked delta-margin facies extend updip into Jefferson County, where sandstone averages 40 percent

of the Lagarto unit. Shelf and transitional faunas dominate.

Depositional patterns within the Oakville map unit are more complex. Most of the sandstone sequence indicates minimal deltaic influence, although the main deltaic depocenter extended to at least the Sabine River. The Oakville coastline was primarily a delta-fringing strandplain consisting of facies assemblages more typical of the barrier/strandplain system. A lower progradational sequence overlain by massive aggradational sand bodies is characteristic (wells MJF-3 through MJF-5, section 1-1', pl. 1). Progradational shoreline sands extend basinward about 10 mi (16 km) into the High Island area. Downdip of this point and extending updip beneath the progradational sandstones as far back as the modern coastline, lenticular, isolated sandstone units locally occur. These sand bodies are completely enclosed within overpressured mudstone (Kiatta, 1971), which contains outer neritic to upper slope faunas (fig. 12), and display blocky to highly serrate log patterns (well MJF-12, section 1-1', pl. 1, for example).

The lithofacies maps show prominent dip-elongate fingers of sandstone extending offshore beneath the High Island area (figs. 10 and 11). These anomalous basal Miocene sandstones are interpreted to be submarine channel fills deposited at the flank of the Calcasieu delta system. Submarine channels commonly occur at the flanks of major delta systems, eroding the upper slope and cutting back into the outer shelf (Burke, 1972; Jackson and Galloway, 1984). Supporting evidence for a submarine channel origin includes their isolation within relatively deep-water marine mudstone sections, the blocky to serrate log patterns (which are typical of slope sands), and their occurrence along narrow dip-oriented belts that extend offshore beyond equivalent shoreline facies. In addition, the sandstones closely resemble the much better described deep-water Hackberry sandstones of the Frio Formation. Further work will be needed to determine the specific relationship of these sands to the contemporaneous lower Miocene strandplain and delta deposits. At this point, we include these submarine channel deposits as a special facies assemblage of the larger delta system.

## Depositional History and Paleogeography

Lithofacies maps and facies interpretations provide a basis for two paleogeographic maps, which offer an overview of the changing coastal plain landscape during deposition of the Fleming episode (fig. 14). Three broad paleogeomorphic provinces compose the landscape: the subaerial coastal plain, the coastline, and the submerged shelf and slope.

Each province was characterized by specific suites of depositional environments and by average declivities of the depositional surface (fig. 15). The coastal plain most likely had a moderately steep gradient, comparable to that of present rivers that originate in or traverse the Edwards Plateau. The shoreline and associated embayments and lagoons formed a broad sea-level surface. Basinward, shelf declivity and width depended upon both depositional setting and position of the shoreline relative to earlier shoreline stands. Following the Anahuac transgression and during later stages of lower Miocene retrogradation, the shelf was relatively broad and possessed moderate to low declivity (fig. 15). The shelf/slope break was probably sharper along the deltaic headlands (see reconstructions of the Quaternary shelf of Texas in Winker, 1979). During active continental margin progradation, the shelf was narrow and the shelf edge ill defined. Slope declivity is conjectural, but a range between  $0.5^\circ$  and  $1.0^\circ$  typifies the present northwest Gulf of Mexico and Niger delta slopes. The Niger is a particularly good analog for a sand-rich, wave-dominated prodelta continental slope unaffected by salt extrusion and diapirism. The lower slope is inferred to be a largely tectonic terrane strongly modified by incipient salt diapirism, toe thrusting, and extrusion of salt and mud.

To the south, the **coastal plain** displayed a relatively steep gradient and was dominated by a braided river system that originated far beyond the basin margin and flowed across Trans-Pecos Texas. Periodic avulsion repeatedly shifted the main channel between two major entry points onto the depositional coastal plain apron. Localization of drainage along the two divergent axes may be speculatively explained by the periodic

diversion or stream capture caused by fault block adjustments along the Balcones or Luling/Charlotte trends. The broad midsection of the coastal plain, which lay basinward of the Balcones Fault Zone and adjoining Edwards Plateau, was traversed by numerous small streams with headwaters in the fringing Cretaceous or older Paleogene outcrops. In East Texas, one or more of the larger meandering basin-fringe rivers traversed a broad, low-relief coastal plain. The largest fluvial system, probably a mixed- or suspended-load drainage complex of continental scale, flowed across central Louisiana; occasionally, however, this system diverted as far west as the easternmost Texas Coastal Plain.

Along the **coastline**, a wave-dominated deltaic headland and associated beach-ridge complex extended across South Texas. However, prominence of this depositional feature decreased during later stages of the Fleming episode. The rest of the Texas coast consisted of an extensive microtidal inter-deltaic bight containing well-developed barrier islands and sandy beach-ridge plains. A broad barrier-island and lagoon complex persisted along the northeast margin of the North Padre delta system. The great thickness of sandstone preserved along this coastal segment indicates that northward longshore drift effectively redistributed much sediment from the deltaic headland, nourishing the barrier complex. Farther northeast, a broad accretionary beach-ridge (strandplain) complex was nourished by numerous smaller streams and their ephemeral deltas as well as by longshore sediment transport from the major deltaic headlands. As retrogradational sedimentation and coastal retreat began to dominate the later history of the early Miocene episode, the barrier-island/lagoon complex expanded to encompass most of the central coastal plain. The western fringe of the Calcasieu deltaic headland and marginal strandplain formed the northeastern boundary of the coastal bight.

Figure 16 illustrates the basic geomorphic elements and sedimentary dispersal dynamics of the lower Miocene coast. Convex deltaic headlands are inherently the focus of wave reworking and divergent longshore transport. In contrast, the coastal bights are a focus for



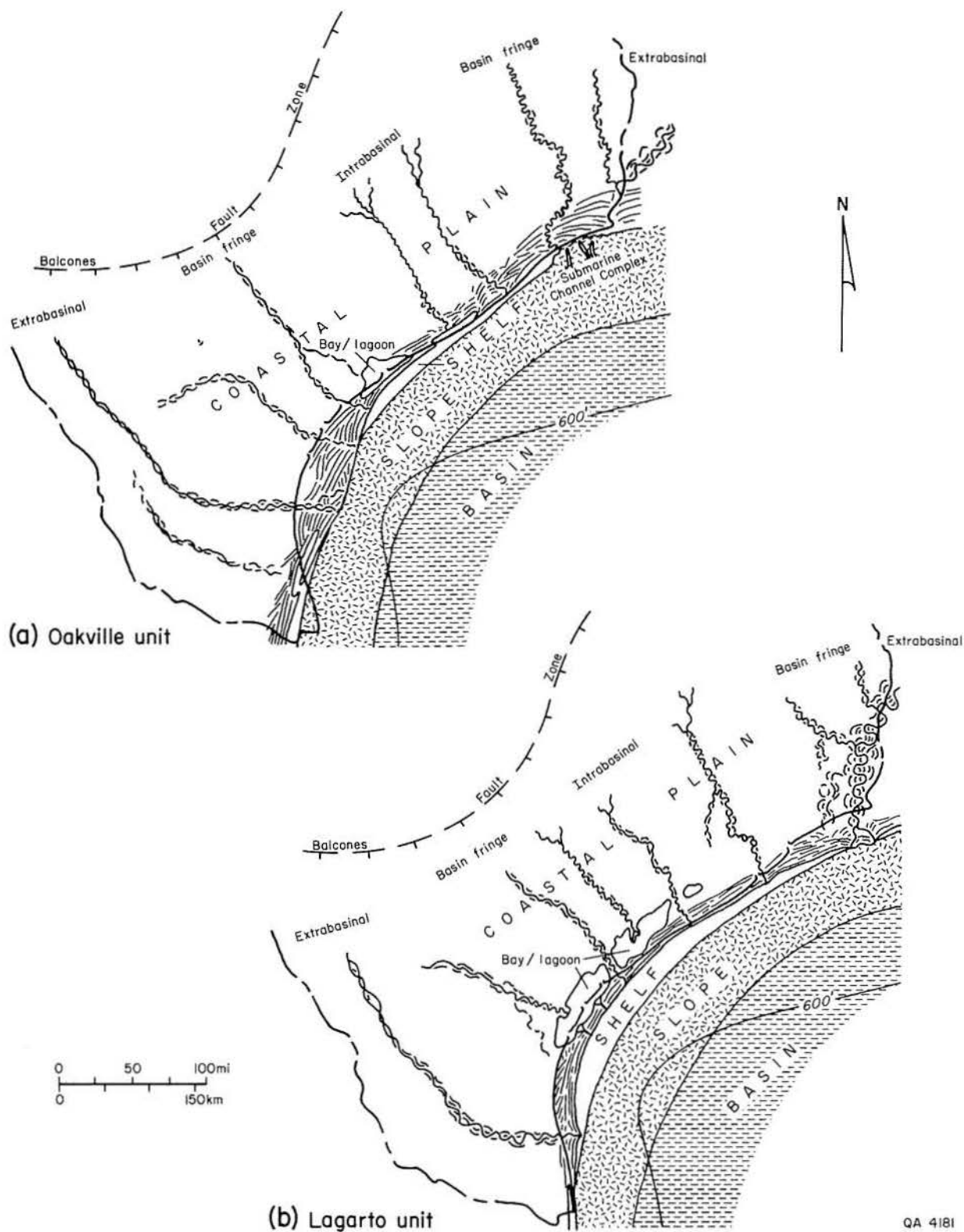


**Figure 14.** Paleogeographic reconstruction during (a) later Oakville progradation and (b) middle Lagarto coastal plain aggradation.



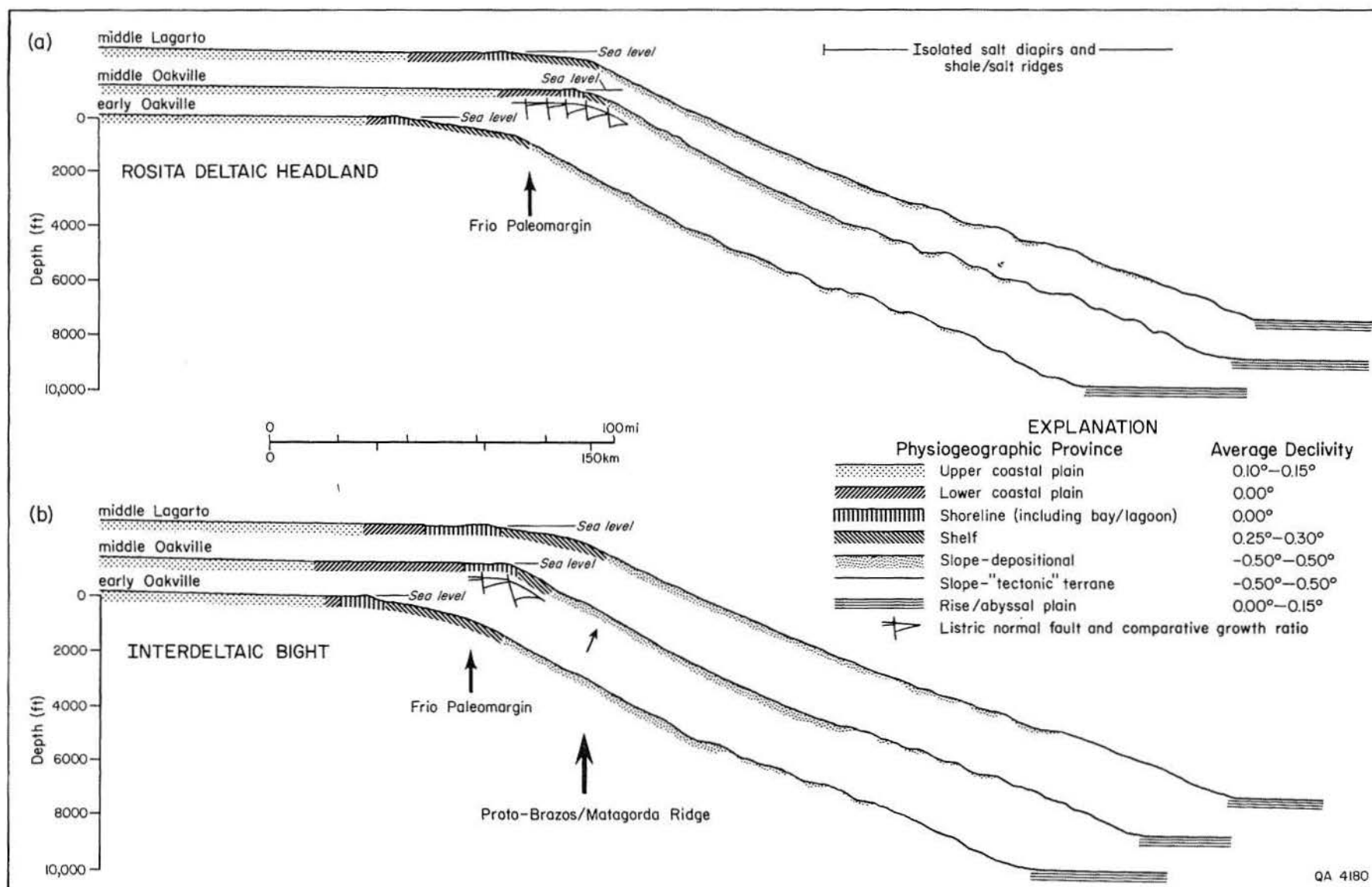


**Figure 15.** Interpretive morphologic profiles across the lower Miocene coastal plain, shoreline, shelf, and slope. The three times selected represent (1) onset of lower Miocene coastal progradation, (2) active progradation of the lower Miocene continental margin, and (3) lower Miocene coastal retrogradation. (a) South Texas Santa Cruz-Rosita fluvial/deltaic headland. (b) Middle Texas interdeltaic bight (Moulton/Point

Blank streamplain and Matagorda barrier/strandplain system). Declivities reflect typical values of comparable settings in the Quaternary Texas Gulf Coast and Nigerian continental margins. The lower Miocene coastal plain is projected updip to the present position of the Fleming outcrop. Widths of the strandline and shelf regimes are based on facies maps and interpreted paleomargin positions.

QA 4180

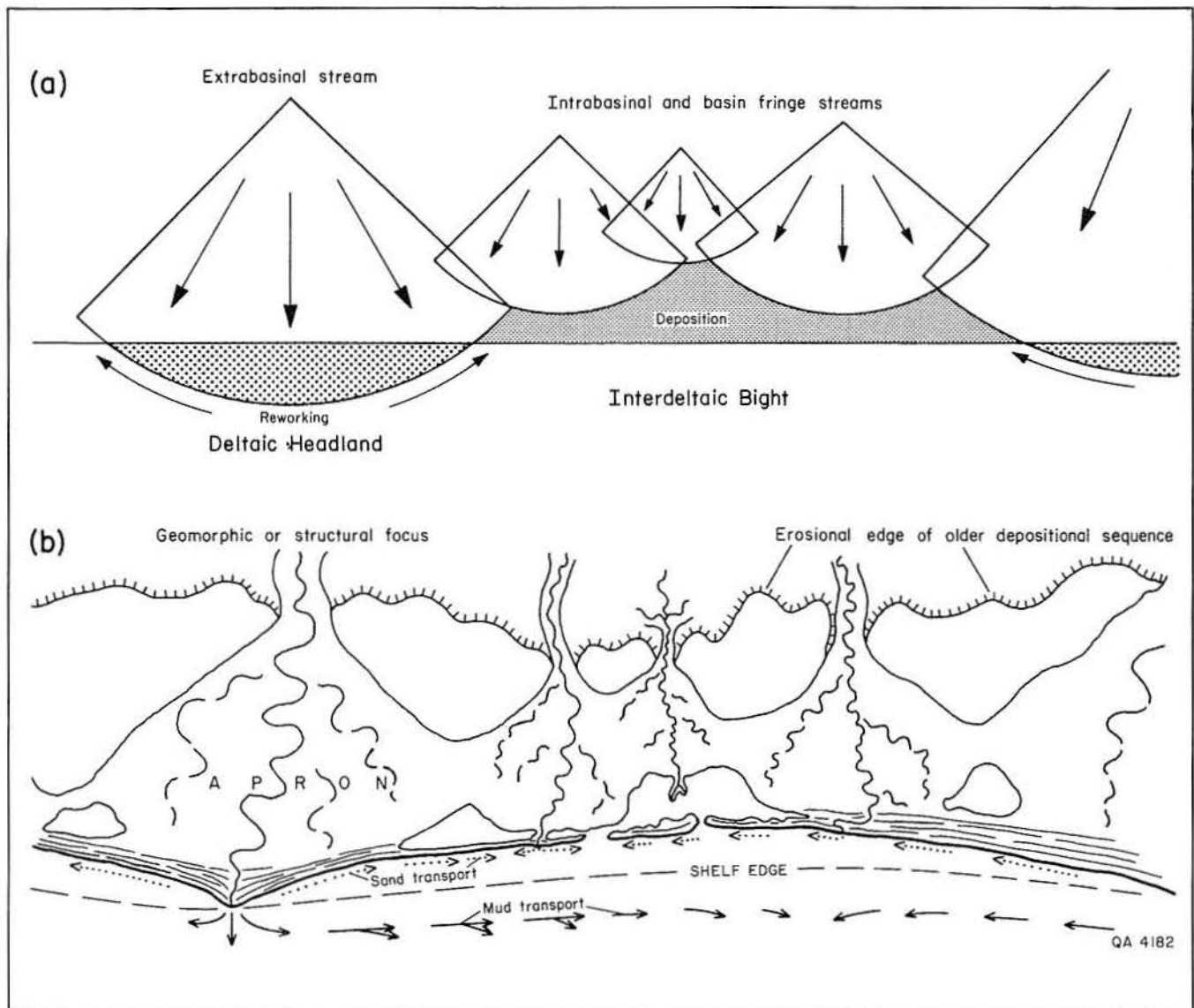


**Figure 16.** Depositional architecture of the lower Miocene coastal plain and shoreline. (a) Schematic drawing of depositional elements indicating principal areas of erosion and redistribution (deltaic headlands) and of deposition (interdeltaic bights). (b) Interpreted lower Miocene depositional environments and sediment dispersal patterns. Drawings modified from Winker (1979).

longshore convergence and deposition (W. A. Price, personal communication, 1978). In strongly wave-dominated shorelines, such as the one that existed during lower Miocene deposition along the Texas coast, large-scale redistribution of sand and mud from the fringe of the fluvial/deltaic apron can shift the ultimate depocenter from the deltaic headland into the interdeltic bight. Sediment loading and resultant flexural down-bowing of the crust induces subsidence of the lower coastal plain. Aggradation of the large fluvial/deltaic aprons

readily keeps up with subsidence, but in interdeltic areas, shallow bays and lagoons may form (fig. 16b). Because principal sediment supply is from the seaward rather than the landward side, relatively stable, well-nourished aggradational barrier and beach-ridge sequences are deposited.

**Shelf and slope** morphology reflected both the long-term history of progradation and transgression as well as the action of marine and coastal processes during the early Miocene. Initially, the lower Oakville coastal

systems prograded onto a broad, transgressively flooded continental shelf platform. However, once Oakville progradation extended to the foundered Frio continental margin, the deltaic headlands built directly onto the upper continental slope (figs. 14a and 15). The interdeltic bight was fronted by a relatively narrow, steeply sloping shelf that graded into the progradational lower Miocene continental slope. Along the western margin of the Calcasieu delta, the shelf was incised by local submarine gullies and gorges. Submarine erosion likely indicates the convergence of

longshore currents along this convex segment of the coastline (Burke, 1972). As the coastline stabilized and locally began to retreat in later Fleming time, continued progradation of the muddy shelf and slope created a broader and better defined shelf (fig. 15). To the northeast, however, the Calcasieu delta rapidly built out to the shelf margin, filling and burying any remaining gorges. Extensive coastal retreat terminating the early Miocene episode again produced a broad, foundered shelf platform upon which the lower *Amphistegina* B shale was deposited.

## ORIGIN AND DISTRIBUTION OF HYDROCARBONS

The lower Miocene depositional sequence is an important oil- and gas-producing unit of the Gulf Coast province. Although the best-known Miocene trend lies within Louisiana (Rainwater, 1964; Curtis, 1970), lower Miocene production extends across most of the Texas Coastal Plain and adjacent continental shelf. This section (1) reviews existing information on the potential sources, generation history, and migration patterns of Miocene oil and gas, (2) inventories and classifies fields into plays, and (3) discusses the potential for undiscovered hydrocarbons in productive or speculative plays.

### Indigenous Source Rocks and Maturation History

Quantitative geochemical data for the lower Miocene operational unit are scanty. Three wells, the Continental Offshore Stratigraphic Test (COST) No. 1 and No. 2 wells (in the South Padre and Mustang Island areas, respectively) and the upper section in the U.S. Department of Energy (DOE)/General Crude Oil (GCO) Pleasant Bayou No. 1 geothermal test well (Brazoria County), provide the only published systematic suites of organic geochemical analyses (Brown, 1980; Huc and Hunt, 1980).

Table 1 summarizes the total organic carbon (TOC) content of sample suites from the three wells. Two facies assemblages are represented. Interbedded prodelta, shelf, and upper slope

mudstones (COST wells) have adequate TOC to qualify as potential source rocks (minimal TOC >0.5 weight percent). Mudstones interbedded with and underlying the strandplain sandstones, penetrated by the DOE/GCO well, are generally lean but exceed the 0.5-weight-percent TOC threshold in a lignitic interval several hundreds of feet thick. Degraded type II and marine type I kerogen would be expected in the marine shales. However, Huc and Hunt (1980) described the organic constituents in the COST wells as being primarily humic (type III). Strandplain mudstones contain a mixture of woody, herbaceous, and amorphous kerogen (Brown, 1980). Nonetheless, pyrolysis experiments yielded significant amounts of hydrocarbon liquids from the COST samples (Huc and Hunt, 1980), and Brown (1980) assigned modest potential oil-generating capacity to the Miocene section in the Brazoria County well. If the data are representative of marine-influenced lower Miocene mud-rock facies, the Fleming depositional sequence contains significantly better source potential than does the underlying, highly productive Frio sequence (Galloway and others, 1982b).

Maturity of the lower Miocene section can be predicted using the generalized Gulf Coast chart prepared by Dow (1978). Assuming that onset of significant oil generation begins at a vitrinite reflectance ( $R_o$ ) value of 0.5, the generation zone would lie between the 240°F (115°C) and 340°F (172°C) isotherms.

**Table 1.** Total organic carbon content of lower Miocene mudstones.  
Data from Brown (1980) and Huc and Hunt (1980).

Well	Facies Assemblage	Weight Percent Average	Total Organic Carbon Range
DOE/GCO Pleasant Bayou No. 1 (Brazoria County)	Strandplain and inner shelf	0.81 (0.46)*	0.14-7.07 (0.14-1.17)*
COST No. 1 (South Padre Island area)	Prodelta and upper slope	0.92	0.72-1.15
COST No. 2 (Mustang Island area)	Outer shelf, prodelta, and upper slope	0.75	0.48-0.97

\* Single anomalously high sample deleted.

Analyses of the COST No. 1 and No. 2 samples are consistent with this prediction. Onset of liquid generation (as determined from results of distillation and pyrolysis techniques) occurs at a present burial temperature of 250° F (120° C) (Huc and Hunt, 1980). This isotherm lies at a depth of about 12,000 ft (3,700 m) in both wells and is associated with measured Ro values of 0.55 to 0.6. Cracking of the heavier hydrocarbons to produce gas is interpreted to begin at a depth of 14,000 ft (4,300 m), at measured Ro values of about 0.8 to 0.9 in the COST No. 1 well.

The 250° F (120° C) isotherm is plotted on each of the three cross sections (pls. 1 through 3). Only deeply buried, distal deposits of the North Padre and Calcasieu delta and the Matagorda barrier/strandplain systems are thermally mature. Indigenous oil or gas generation thus appears to be limited to the lower Miocene expansion zone, basinward of the Frio paleomargin.

## Migration and Entrapment

Mechanisms of primary expulsion and migration of hydrocarbons generated within the Gulf Coast Cenozoic fill are poorly documented. Discussion of principal theories is beyond the needs of this report. However, a few constraints and patterns widely recognized

in other producing units appear to be equally valid for the lower Miocene sequence.

Thermal maturation and resultant oil and gas generation occur within the overpressured section (Morton and others, 1985a). Downdip, prodelta, shelf, and upper slope facies of the Miocene, as well as of other Gulf Coast Cenozoic episodes, are ubiquitously geopressured (Wallace and others, 1981). Thus fluid pressure gradients favor an upward migration of formation waters and dissolved or associated hydrocarbon fluids. Galloway and others (1982c) showed that distribution of oil and gas pools within the Frio Formation indicates a minimum vertical migration of several thousand feet and that principal producing trends are closely associated with regional structures—salt domes and major growth fault zones—that provided potential conduits for such migration.

The geochemical data of Huc and Hunt (1980) provide evidence of migration of light hydrocarbon fractions upward from the zone of generation within the lower Miocene section of the COST No. 1 well. Here, migration, which appears to have been either by diffusion or by solution entrainment in expelled formation waters, was as much as 2,000 ft (600 m).

Rice (1980) used carbon isotope data to show that deep Miocene nonassociated gases of the offshore trend are the product of either



late-stage methanogenesis of kerogen or thermal cracking of previously generated oil. Because thermal generation of gas occurs below the oil generation window (probably at depths exceeding 14,000 ft [4,300 m]), vertical migration from source to reservoir must extend at least several thousand feet. Fractionation during this migration would explain the occurrence of much of the thermogenic gas in nonassociated dry gas pools (Rice, 1980).

## Occurrence of Oil and Gas

The spatial distribution of commercial hydrocarbon pools in the lower Miocene depositional sequence will be described in the context of play analysis. White (1980) defined a play as a geologically homogeneous subdivision of the universe of hydrocarbon pools within a basin. Typically, fields within a play share common hydrocarbon type, reservoir genesis, trapping mechanism, and source. Steps in defining and describing lower Miocene plays were as follows:

(1) All fields that have produced more than 1 million barrels of oil equivalent (boe) (1 boe = 6 Mcf of gas) were examined and lower Miocene reservoirs isolated. Where production from lower Miocene reservoirs in the field exceeded the 1-million-boe threshold, basic data on cumulative production, reservoir depths, and hydrocarbon types were tabulated, providing a hydrocarbon inventory. Production figures were taken from the 1982 Annual Report of the Railroad Commission of Texas (RRC) for onshore areas. For offshore areas, where the history of exploration and production is generally less extensive, production figures compiled through June 1984 by the RRC were used.

(2) All fields meeting the minimum production criteria were indicated on a regional base map (fig. 17).

(3) The energy equivalencies of total liquids and gas production, in boe, were calculated and indicated on the map by proportional shading of the field area (fig. 17). This highlights similarities of produced hydrocarbon type.

(4) Larger reservoirs within the fields were projected into adjacent dip cross sections at the

appropriate stratigraphic level (as shown in pls. 1 through 3) to illustrate any patterns in vertical distribution of oil and gas pools.

(5) Finally, the quantitative and qualitative production data were analyzed within the context of the geologic framework to define and delimit a coherent set of plays.

## General Features of Lower Miocene Plays

Reservoirs deposited during the lower Miocene episode have produced nearly 2.7 billion barrels (bbl) of oil and condensate and more than 5 Tcf of gas (including casinghead gas, for which records are, at best, incomplete). This totals more than 3.5 billion boe, making the lower Miocene of the Texas coast a major producing unit of the Gulf Coast Basin, though certainly not one of the largest. An unknown additional volume of oil and gas has been produced by smaller fields that have produced less than 1 million boe. However, Galloway and others (1982b) found that in the Frio Formation such smaller fields account for only a small percentage of total production. Thus, we are confident that the larger fields considered in this study represent the bulk of lower Miocene production. Comparatively young fields of the Federal Outer Continental Shelf (OCS) may ultimately add significantly to these totals, but, as will be shown, they now contribute only modestly.

Lower Miocene production is grouped into nine plays, which are delineated in figure 17. Fields included in each play are listed in the appendix. Salient attributes of each play are given in table 2. Volumetric parameters for each play, including produced hydrocarbons and lithologic content, are given in table 3. Finally, comparative productivity of each play is shown in figures 18 and 19.

In addition to summary data for each play, which are best shown by graphics or tables, several general observations are noteworthy:

(1) Only plays I through IV contain indigenous, thermally mature lower Miocene source mudstones. Ironically, some of the best, richest, and most oil-prone of all described Cenozoic source rocks are found within gas plays that have proved thus far to be comparatively poor producers.

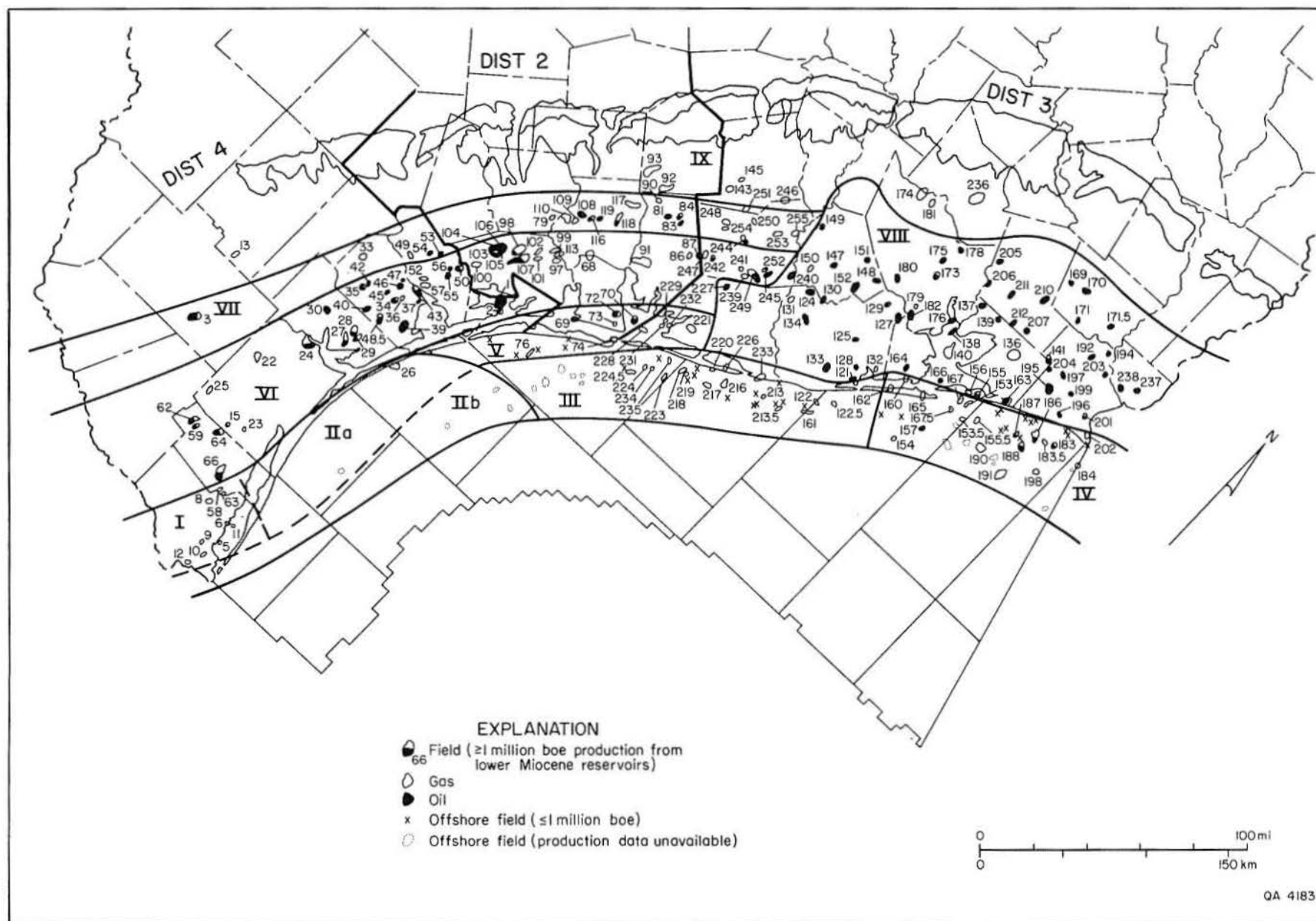


**Figure 17.** Distribution of lower Miocene oil and gas fields that have produced more than 1 million boe of hydrocarbons. Nine identified plays are outlined and designated with roman numerals. Numbers shown by fields correspond to field identification numbers in appendix.

**Table 2.** Summary of geologic characteristics and remaining potential of lower Miocene oil and gas plays.

<b>Play I</b>	
<b>Hydrocarbon Type(s):</b>	Dry gas.
<b>Defining Attribute(s):</b>	Small growth-fault traps along southern margin of North Padre delta system; reservoirs concentrated in Fleming operational unit, near <i>Amphistegina</i> B shales.
<b>Reservoir Genesis:</b>	Distal delta and delta-destructural sandstones.
<b>Structural Style:</b>	Reactivated Frio and Anahuac growth faults.
<b>Trapping Mechanisms:</b>	Growth-fault-related structure, including upthrown blocks.
<b>Possible Hydrocarbon Source(s):</b>	Subjacent Frio/Anahuac slope and prodelta mudstone; possibly interbedded and subjacent lower Miocene shelf mudstone.
<b>Exploration Maturity:</b>	Immature to mature.
<b>Frontiers:</b>	Deep lower Miocene; extension offshore along trend into area of play IIa.
<b>Limitations:</b>	1. Gas-prone, low-quality source rocks. 2. Small field size.

<b>Play IIa</b>	
<b>Hydrocarbon Type(s):</b>	Gas and condensate.
<b>Defining Attribute(s):</b>	North Padre delta system overlying distal Frio deltaic platform.
<b>Reservoir Genesis:</b>	Various progradational and aggradational, wave-dominated delta-margin sandstone facies.
<b>Structural Style:</b>	Reactivated Frio and Anahuac growth faults and shale ridges.
<b>Trapping Mechanisms:</b>	Growth-fault-related structure.
<b>Possible Hydrocarbon Source(s):</b>	Subjacent Frio/Anahuac slope and prodelta mudstone.
<b>Exploration Maturity:</b>	Immature.
<b>Frontiers:</b>	Entire play sparsely drilled.
<b>Limitations:</b>	1. Poor seal development. 2. Gas-prone, low-quality source in underlying thermally mature Frio section.

<b>Play IIb</b>	
<b>Hydrocarbon Type(s):</b>	Gas and condensate.
<b>Defining Attribute(s):</b>	Progradational continental margin of North Padre delta system and subjacent upper slope.
<b>Reservoir Genesis:</b>	Progradational and aggradational wave-dominated delta-margin sandstones; possible upper slope sandstone units.
<b>Structural Style:</b>	Large-scale growth faults of an extensional continental margin stress regime; subjacent shale ridges.
<b>Trapping Mechanisms:</b>	Dip reversal, rollover, and truncation associated with active growth faults and shale ridges.
<b>Possible Hydrocarbon Source(s):</b>	Subjacent Frio/Anahuac and interbedded prodelta, shelf, and slope mudstone.
<b>Exploration Maturity:</b>	Immature.
<b>Frontiers:</b>	Entire play sparsely drilled.
<b>Limitations:</b>	1. Gas-prone production. 2. Complex, discontinuous structural trends. 3. Degradation of reservoir quality by burial diagenesis.

<b>Play III</b>	
<b>Hydrocarbon Type(s):</b>	Gas and minor amounts of condensate.
<b>Defining Attribute(s):</b>	Gas fields in down-faulted shore-zone and shelf facies of the Matagorda barrier/strandplain system capping the lower Miocene offlap continental margin.
<b>Reservoir Genesis:</b>	Shoreface, inner-shelf, and subordinate barrier-core and beach-ridge sand bodies of a microtidal shore-zone system.
<b>Structural Style:</b>	Large-scale growth faults of an extensional continental margin stress regime. Major listric faults are concentrated along a narrow strike-parallel and continuous zone.
<b>Trapping Mechanisms:</b>	Prominent rollover, dip reversal, and offset associated with growth faults and adjacent shale ridges.
<b>Possible Hydrocarbon Source(s):</b>	Subjacent Frio/Anahuac and possibly interbedded shelf and slope mudstones.
<b>Exploration Maturity:</b>	Mature to immature.
<b>Frontiers:</b>	Deeply buried reservoirs in downdropped fault blocks; southward continuation into sparsely drilled Federal OCS.
<b>Limitations:</b>	1. Abrupt basinward decrease in sand content. 2. Intrusion of large shale ridge along basinward margin of play.

<b>Play IV</b>	
<b>Hydrocarbon Type(s):</b>	Gas and minor amounts of oil.
<b>Defining Attribute(s):</b>	Progradational continental margin of the Calcasieu delta system and its adjacent delta-flank strandplain and subjacent slope.
<b>Reservoir Genesis:</b>	Progradational and retrogradational strandplain shoreface and delta-front sandstone facies; sandy fills of upper slope erosional(?) channels.
<b>Structural Style:</b>	Complex growth faults of an extensional continental margin stress regime. Shale ridges along basinward margin; salt diapirs along updip margin.
<b>Trapping Mechanisms:</b>	Growth-fault and salt-related structures.
<b>Possible Hydrocarbon Source(s):</b>	Subjacent Frio/Anahuac slope and interbedded slope, shelf, and prodelta mudstones.
<b>Exploration Maturity:</b>	Mature.
<b>Frontiers:</b>	Deeply buried slope gorge fills and downfaulted distal-shoreface and delta-front sandstone trends.
<b>Limitation:</b>	1. Basinward and downward decrease in sand content.

<b>Play V</b>	
<b>Hydrocarbon Type(s):</b>	Gas and minor amounts of oil.
<b>Defining Attribute(s):</b>	Mixed structural and stratigraphic traps along updip transition of massive Oakville barrier/strandplain sandstones into lagoon and coastal plain mudstone.
<b>Reservoir Genesis:</b>	Back-barrier and beach-ridge sand bodies, particularly of upper part of lower Miocene episode.
<b>Structural Style:</b>	Reactivated Frio growth and antithetic faults and associated rollover and dip reversal.
<b>Trapping Mechanisms:</b>	Mixed structure and stratigraphic updip sand pinch-out.
<b>Possible Hydrocarbon Source(s):</b>	Underlying Frio and older shelf and slope mudstones.
<b>Exploration Maturity:</b>	Mature.
<b>Frontiers:</b>	Inner continental shelf along south end of play.
<b>Limitations:</b>	1. Lack of indigenous mature source rocks. 2. Onshore area densely drilled.



**Table 2 (cont.)**

<b>Play VI</b>	
<b>Hydrocarbon Type(s):</b>	Subequal amounts of oil and gas.
<b>Defining Attribute(s):</b>	Shallow subaerial coastal plain fluvial and subjacent delta and shore-zone reservoirs productive over or updip of reactivated Frio growth-fault trends; commonly superimposed on Frio fields.
<b>Reservoir Genesis:</b>	Mixed deltaic, shore-zone, and fluvial sand facies of several depositional systems.
<b>Structural Style:</b>	Low-relief structures associated with reactivated Frio fault zones.
<b>Trapping Mechanisms:</b>	Structural and combination traps related to prominent Frio fault zones.
<b>Possible Hydrocarbon Source(s):</b>	Leakage from underlying Frio reservoirs or directly from deeply buried Frio or older mudstones.
<b>Exploration Maturity:</b>	Supermature to mature.
<b>Frontiers:</b>	None.
<b>Limitations:</b>	1. Existing well density. 2. Lack of mature, indigenous source.

<b>Play VII</b>	
<b>Hydrocarbon Type(s):</b>	Gas and oil.
<b>Defining Attribute(s):</b>	Shallow fields aligned along and updip of the Vicksburg fault zone; commonly superimposed on shallow Frio reservoirs.
<b>Reservoir Genesis:</b>	Fluvial sandstones.
<b>Structural Style:</b>	Low-relief folds and minor fault offset inherited from deeply buried fault zones.
<b>Trapping Mechanisms:</b>	Low-relief structural traps.
<b>Possible Hydrocarbon Source(s):</b>	Leakage from underlying Frio reservoirs or injection along fault zones from Paleogene marine shales.
<b>Exploration Maturity:</b>	Supermature.
<b>Frontiers:</b>	None.
<b>Limitations:</b>	1. Existing well density. 2. Thin, shallow section.

<b>Play VIII</b>	
<b>Hydrocarbon Type(s):</b>	Oil and subordinate gas.
<b>Defining Attribute(s):</b>	Oil-prone fields found in or around salt domes of the Houston salt diapir province.
<b>Reservoir Genesis:</b>	Fluvial, deltaic, and shore-zone sand bodies of several adjacent depositional systems.
<b>Structural Style:</b>	Deep and shallow piercement salt domes and associated fault systems.
<b>Trapping Mechanisms:</b>	Structural traps above and flanking domes.
<b>Possible Hydrocarbon Source(s):</b>	Injection from deep Eocene(?) sources along dome-related tensional structures.
<b>Exploration Maturity:</b>	Supermature to mature.
<b>Frontiers:</b>	None.
<b>Limitations:</b>	1. Existing well density.

Play IX	
Hydrocarbon Type(s):	Dry gas.
Defining Attribute(s):	Very shallow gas fields scattered within updip fluvial deposits.
Reservoir Genesis:	Fluvial sandstones.
Structural Style:	Low-relief terracing and folding; minor fault displacement along reactivated deep-seated growth-fault trends.
Trapping Mechanisms:	Low-relief structural, combination, or stratigraphic(?) traps.
Possible Hydrocarbon Source(s):	Leakage from underlying reservoirs(?).
Exploration Maturity:	Supermature.
Frontiers:	None.
Limitations:	1. Thin, shallow, densely drilled section. 2. Active meteoric circulation.

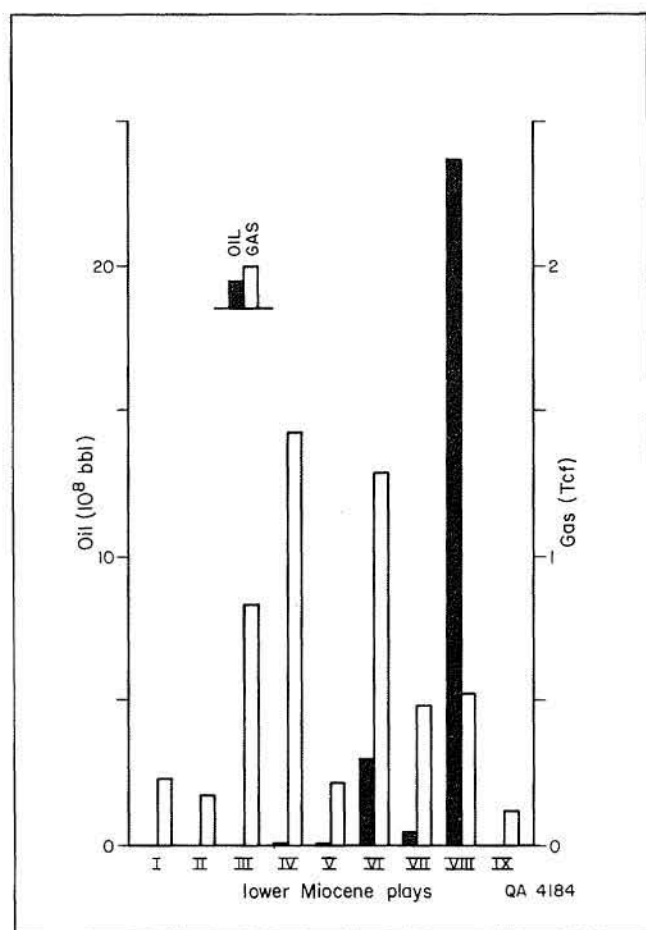


**Figure 18.** Cumulative oil and gas production for each of the nine lower Miocene plays.

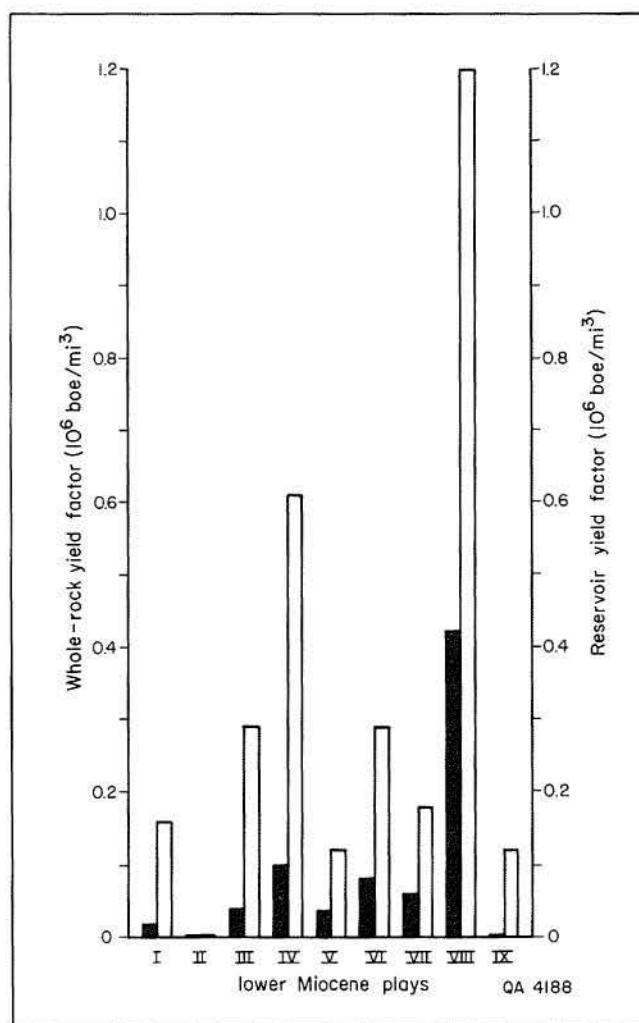


**Figure 19.** Total hydrocarbon yield factors calculated on the basis of estimated total rock volume and total sandstone volume contained within each of the nine Miocene plays. Units are boe/mi<sup>3</sup>.

**Table 3.** Cumulative production and sedimentary volumes of lower Miocene plays. Compiled from annual reports and unpublished tabulations of the Railroad Commission of Texas.

Play	Hydrocarbon Production			Play Volumetrics			Yield Factor	
	Oil (10 <sup>6</sup> bbl)	Gas (10 <sup>6</sup> Mcf)	Condensate (10 <sup>6</sup> bbl)	Total boe (10 <sup>6</sup> )	Area (mi <sup>2</sup> )	Whole-Rock Volume (mi <sup>3</sup> )	Reservoir Volume (mi <sup>3</sup> )	Average Percent Sandstone
I	0	226	0.2	38	950	1,060	230	22
II	0	17	0.7	4	3,980	5,590*	930*	17
III	0	824	2.2	140	3,370	3,650*	480*	13
IV	8	1,426	4.1	250	2,260	2,920*	410*	14
V	7	214	0.1	43	1,550	1,370	350	26
VI	286	1,290	0.7	501	8,300	6,020	1,730	29
VII	38	472	<0.1	117	4,730	1,930	640	33
VIII	2,341	518	1.1	2,428	9,100	5,800	2,020	35
IX	<1	108	<0.1	18	14,780	3,950*	1,540*	39
<b>Total</b>	<b>2,680</b>	<b>5,095</b>	<b>9</b>	<b>3,539</b>	<b>49,020</b>	<b>31,760</b>	<b>8,330</b>	<b>26</b>

\* Extrapolations based on area of play mapped.

(2) Relative play richness is best compared by use of yield factors—the volume of produced hydrocarbons relative to the total sediment or total reservoir volume within each play. As emphasized by White (1980), reservoir distribution (the presence of significant volumes of sandstone) is a common limitation, particularly in downdip plays of the Gulf Coast. We concur that production per unit volume of sandstone provides one of the best indices for comparison of play richness or prediction of ultimate potential. As shown in figure 19, play VIII is by far the most productive increment of the Fleming episode.

(3) The adage that Gulf Coast salt dome provinces are optimum sites for petroleum and particularly for oil entrapment is again demonstrated. Play VIII, which is by definition delimited by the Houston salt basin, has produced nearly 90 percent of the oil and more than 65 percent of all hydrocarbons recovered from the lower Miocene.

(4) The important updip plays (VI through IX) are generally coincident with analogous plays delineated by Galloway and others (1982b) in the Frio Formation. The highly productive play VIII coincides with three comparably oil-prone Frio plays. Plays V, VI, and VII are most productive over the Frio barrier/strandplain system, which hosts two of the most productive Frio plays (Galloway and others, 1982b). Many of the fields shown in figure 17 also produce from multiple Frio reservoirs. Typically, Frio production exceeds that of the Miocene zones. In effect, the lower Miocene seems to have collected the leakage or overflow from the richer Frio plays.

(5) The pervasive vertical migration of hydrocarbons into shallower reservoirs commonly produces multipay fields and blurs association of hydrocarbons with any particular facies assemblage or even any depositional system. Each lower Miocene depositional system contains potential reservoir and sealing facies; consequently, all produce. Where present, progradational and retrogradational delta-front and shoreline sandstone units typically constitute a prominent reservoir facies, particularly if interbedded with marine mudstones. Obvious geographic trends of field distribution patterns,

as seen in parts of plays VI and VII, are closely related to major structural features (in these examples, the Vicksburg and Frio fault zones).

## Exploration Potential

Because of their divergent exploration histories, lease acquisition procedures, and production economics, the onshore area and adjacent State submerged lands and the Federal OCS present two somewhat different problems in assessment of undiscovered recoverable hydrocarbons. DuBar (1983) made initial projections of undiscovered lower Miocene oil and gas in the three RRC districts that encompass the coastal plain and the State submerged lands. Foote (1984) evaluated Texas OCS potential, and Morton and others (1985a) provided a qualitative assessment of the major offshore trends of the Texas shelf.

### Onshore and State Submerged Lands

Galloway and others (1982b) used three historical approaches to project volumes of undiscovered recoverable hydrocarbons in RRC Districts 2, 3, and 4 as of 1977. The first method plots discovery rate against the cumulative number of exploratory wells. Ultimate reserves are assumed to be tapped when drilling reaches a certain density, which was arbitrarily defined as 2 wells per  $\text{mi}^2$ . The second method plots the volumes of oil and gas discovered against total exploratory well drilling footage. We assumed in making the projection that a maximum total footage of 15,000 ft (4,500 m) per  $\text{mi}^2$  will be required for thorough testing of the section. Finally, the third approach projects ultimate discovery by extrapolating the discovery versus time curve for each of the districts. This approach proved least satisfactory because determination of the discovery peak that defines one-half of ultimate reserves using data disaggregated to RRC district level is arbitrary. Details of the projection procedures were reviewed in Galloway and others (1982b) and will not be repeated here.

Projections for each district made on the basis of these three methods are summarized in table 4. Finding rates in recent years are so low

that the figures generated from 1977 statistics remain little reduced. DuBar (1983) estimated the portion of the total for each district that might reasonably be assigned to discovery in lower Miocene plays by assuming that historical production predicts the fraction of remaining potential belonging to each stratigraphic unit. As can be seen in table 4, lower Miocene reservoirs account for only a modest percentage of total production in Districts 2 and 4. However, play VIII is a major production component in upper coastal plain District 3. The projections indicate that noteworthy additional reserves, totaling more than 100 million bbl of oil and 10 Tcf of gas, probably remain in lower Miocene reservoirs, mainly in play VIII and adjacent parts of plays III and IV that extend into State submerged lands.

### Outer Continental Shelf

Outer Continental Shelf reserves of the western Gulf Coast Basin are concentrated in the Plio-Pleistocene trend. Salt-related structural traps of this trend contain 91 percent of the oil and 75 percent of the gas reserves in the Texas OCS (Morton and others, 1985a). It is uncertain whether this figure reflects ultimate distribution of reserves, but the historical domination of salt diapir provinces (as exemplified by the lower Miocene depositional episode itself) suggests that the proportions are likely to remain good indices for disaggregating the projected undiscovered reserves of the Texas OCS summarized in Foote (1984). Foote's mean estimated values of 640 million bbl and 15.5 Tcf yield projections of 64 million bbl of oil and nearly 4 Tcf of gas remaining to be discovered in OCS Miocene reservoirs. Most of the oil and perhaps half of the gas may be assigned to lower Miocene plays.

The U.S. Minerals Management Service tabulated by area estimated recoverable reserves in Miocene fields of the Federal OCS. Upper Miocene fields of the Brazos area and the uniquely large Buccaneer field (mostly upper Miocene production) of the Galveston area can be excluded from this tabulation. Size distribution of the remaining 32 OCS fields (which are mostly within lower Miocene plays II, III, and IV) is illustrated in figure 20. The



**Table 4.** Projected volumes of undiscovered recoverable hydrocarbons (million bbl and Tcf) by Railroad Commission district as of 1977 (from Galloway and others, 1982b; DuBar, 1983).

Location	To be discovered for drill density of 2 wells/mi <sup>2</sup>		To be discovered for cumulative exploratory well footage of 15,000 ft/mi <sup>2</sup>		To be discovered according to projection of decline from interpreted peak discovery		Approximate proportion of total district production attributed to lower Miocene reservoirs	
	Oil	Gas	Oil	Gas	Oil	Gas	Oil	Gas
District 2	50	3	83	5	482	5	1	3
District 3	410	94	553	104	1,172	6	32	14
District 4	169	9	265	15	573	19	4	3

dominant contribution of the medium-sized (8 through 64 million boe) fields to total reserves is apparent. Thus, exploration history suggests that future discoveries will be concentrated in this medium- to small-sized range. However, discovery of even a single large field could dramatically increase the total lower Miocene reserves, which are estimated at about 450 million boe. Thirty percent of Miocene reserves are contained in only two fields.

Lower Miocene plays with substantial extensions into the Federal OCS are II, III, and IV (fig. 17). In comparison with shallow-water and onshore plays, drilling density is relatively low in these plays. In addition, potential lower Miocene reservoirs occur at moderate to great depths, and many of the wells do not penetrate the entire sand-bearing section. Thus, exploration potential here may be considered to be more open ended. To date, however, drilling reflects in part economic limitations to offshore gas production from small- to medium-sized fields. Furthermore, exploration has been made on the basis of systematic seismic investigation of structure and has utilized increasingly sophisticated technology. Thus, one may argue that fewer wells adequately test offshore targets.

Possible exploration frontiers within each play are briefly reviewed in table 2. The open-ended offshore plays warrant additional comment.

**Play II** is, in many ways, a speculative continuation across Mustang, North Padre, and South Padre Island areas of the downdip lower

Miocene gas-productive trend. Few producing fields are delineated, and little production history is available. Total recoverable reserves are estimated to be about 50 million boe in OCS fields. Net-sandstone maps (figs. 8 and 10) reveal the presence of great thicknesses of sandstone within both the Lagarto and Oakville operational units. The play is further tentatively subdivided into two segments, IIa and IIb (table 2). Aggradational delta-plain and coastal-barrier sandstones dominate segment IIa. Structure is largely inherited from the underlying Frio deltaic platform. In contrast, segment IIb consists of several thousand feet of progradational delta-front sandstone and interbedded prodelta, shelf, and upper slope mudstone (pl. 3) deposited in the narrow Miocene expansion zone seaward of the Frio paleomargin. Expansion ratios and structural relief are thus greater in this segment. A depocenter containing more than 1,500 ft (450 m) of sandstone, centered in the eastern Mustang Island area (fig. 8), offers a particularly promising target in play IIb. Optimism must be tempered, however, by the fact that the underlying Frio delta complex has thus far proved a mediocre producer (as have onshore lower Miocene deltaic deposits at the south end of play VI) in the same area. Furthermore, the mineralogic immaturity of lower Miocene sandstones may presage problems of reservoir quality in deeply buried sections.

**Play III** is being extended along strike into the Mustang Island area by recent drilling from its initial development area in State waters

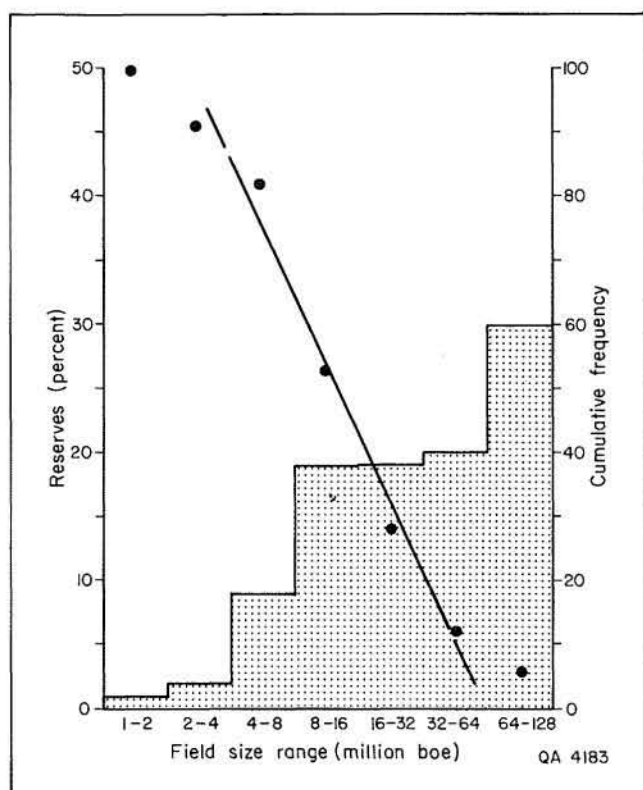


**Figure 20.** Distribution of total producible reserves in 32 Miocene fields in Federal OCS areas. Obvious middle and upper Miocene fields were excluded, but some such tracts most likely remain in the data set. Their inclusion, however, would probably not significantly modify the reserve distribution patterns.

(fig. 17). The potential for numerous additional discoveries along this trend is considered to be good, particularly because such delta-flank positions have proved especially productive in other Gulf Coast units, such as the Frio. Further possibilities for reserve additions include

testing of distal shoreface and inner-shelf sandstones caught up in lower Miocene continental margin faults. The deep, overpressured Frio gas reservoirs in Nueces Bay provide a working analog (Jackson and Galloway, 1984). However, the abrupt decrease in sandstone content seaward of the barrier/strandplain axis limits the dip width of the play, particularly in the Brazos and Galveston areas.

**Play IV** is the most mature of the offshore plays. Producing reserves in the Federal OCS tracts are estimated to be 325 million boe, and reserves of three fields exceed 50 million boe, making this the most prolific area of lower Miocene production. Deltaic and shoreline sandstones have some additional potential, but obvious structures are generally tested. More speculative is the possible extension of the play downdip along the dip-oriented slope trough fills, for which limits have not been established by existing wells (fig. 8). Although sandstone percentage is low and the section is deep, comparable overpressured reservoirs are already productive within the play. Along with distal delta-front sandstones of the Lagarto interval, sandstones in the Oakville submarine channel fills provide deep-drilling targets that could significantly increase the productivity of this most productive of the downdip lower Miocene plays.

The basinward economic limit of the OCS plays is drawn at the lower Miocene paleomargin. Beyond this margin, distal delta, shelf, and slope facies abruptly descend beneath the thick wedge of younger Miocene deposits.

## CONCLUSIONS

(1) Deposits of a distinct lower Miocene depositional episode can be recognized in the Northwest Gulf Coast Basin. The depositional sequence of this episode is bounded by the Anahuac and *Amphistegina* B transgressive marine shale tongues and contains an important but less extensive shale tongue, the *Marginulina* a. shale. The sequence exhibits subequal progradational (lower) and aggradational retrogradational (upper) components.

The shift from progradational to retrogradational sedimentation influenced the depositional style of updip fluvial systems, allowing subdivision of the depositional complex into upper and lower operational map units. These units approximate the Oakville and Lagarto Formations of the outcrop.

(2) Lower Miocene deposits record a major transition in the depositional history of the Gulf of Mexico. The principal deltaic depocenter

shifted from the Rio Grande Embayment, where it had persisted throughout Oligocene time, to the Mississippi Embayment. At the same time, numerous small streams, which drained the rising Edwards Plateau, transported large volumes of locally derived sediment across the Texas Coastal Plain.

(3) Lower Miocene structural features are typical of the Gulf of Mexico Cenozoic fill. A narrow expansion zone developed where deposition prograded beyond the underlying Frio paleocontinental margin. This zone was dominated by an extensional stress regime and resultant listric normal faulting. Depositional loading induced flow of deeply buried, overpressured slope mud. However, the thickness of Mesozoic salt was inadequate to induce active salt diapirism beneath the lower Miocene coastal plain, shelf, and upper slope.

(4) Principal depositional elements of the lower Miocene episode are the diminished South Texas fluvial (Santa Cruz) and wave-dominated (North Padre) delta systems and the prominent barrier/strandplain (Matagorda) system fronting a broad coastal plain traversed by many local streams. Only the western fringe of the principal lower Miocene fluvial and delta

depocenter, which is centered in the Mississippi Embayment, extends into the study area.

(5) The lower Miocene of Texas is an important but not a giant petroleum producing sequence. Total production approaches 4 billion boe. This total is dominated by oil and gas found in the Houston salt dome province. Downdip, offshore plays are estimated to have contained more than 450 million boe of original recoverable reserves, mostly gas.

(6) The potential of the offshore lower Miocene sequence reflects a balance of favorable and unfavorable factors. Potential reservoir sandstone facies are abundant beneath most of the inner continental shelf. Both inherited and contemporaneous structures could produce numerous traps. Sparse data indicate that indigenous source rocks are of fair to good quality and are thermally mature in deeply buried mudstones of the Miocene expansion zone. Finally, large volumes of section are only sparsely drilled. However, the history of Miocene production in nonsalt areas is one of mediocre productivity from numerous, but small, gas fields.

## ACKNOWLEDGMENTS

Funding for this project was provided in part by the Minerals Management Service, U.S. Department of the Interior, under agreement numbers 14-12-0001-30115 and 14-12-0002-40029. Specifically, agreement number 14-12-0001-30115 supported work reported in the section titled "Origin and Distribution of Hydrocarbons," and agreement number 14-12-0002-40029 supported the research program reported in the rest of this publication. This funding is gratefully acknowledged.

The manuscript benefited from technical review by and discussions with Jules R. DuBar,

Shirley P. Dutton, Robert J. Finley, Michael A. Fracasso, and Noel Tyler. Word processing was by Rosanne M. Wilson and typesetting was by Lola E. Huitt, under the supervision of Lucille C. Harrell. Figures were drafted by Richard M. Platt and plates were drafted by John T. Ames, under the supervision of Richard L. Dillon. Margaret L. Evans designed the cover and text for this report. Text illustration camerawork was by James A. Morgan. Editing was by R. Marie Jones-Littleton and Mary Ellen Johansen.



## REFERENCES

- Barnes, V. E., 1974, Austin sheet: The University of Texas at Austin, Bureau of Economic Geology, Geologic Atlas of Texas, scale 1:250,000.
- Brown, S. W., 1980, Hydrocarbon source facies analysis, Department of Energy and General Crude Oil Company Pleasant Bayou No. 1 and 2 wells, Brazoria County, Texas, in Dorfman, M. H., and Fisher, W. L., eds., Proceedings, 4th U.S. Gulf Coast Geopressured-Geothermal Energy Conference: The University of Texas at Austin, Center for Energy Studies, v. 1, p. 132-148.
- Bruce, D. H., 1973, Pressured shale and sediment deformation: mechanism for development of regional contemporaneous faults: American Association of Petroleum Geologists Bulletin, v. 57, p. 878-886.
- Burke, K., 1972, Longshore drift, submarine canyons, and submarine fans in development of Niger delta: American Association of Petroleum Geologists Bulletin, v. 56, p. 1975-1983.
- Caughey, C. A., 1981, Deltaic and slope deposits in the Planulina trend (basal Miocene), southwestern Louisiana (abs.), in Recognition of shallow-water versus deep-water sedimentary facies in growth-structure affected formations of the Gulf Coast Basin: Society of Economic Paleontologists and Mineralogists, Gulf Coast Section 2d Annual Research Conference, Abstracts, p. 20-21.
- Chapin, C. E., 1979, Evolution of the Rio Grande rift—a summary, in Riecker, R. E., ed., Rio Grande rift: tectonics and magmatism: Washington, D.C., American Geophysical Union, p. 1-5.
- Crans, W., Mandl, G., and Haremboure, J., 1980, On the theory of growth faulting, a geomechanical delta model based on gravity sliding: Journal of Petroleum Geology, v. 2, p. 265-307.
- Curtis, D. M., 1970, Miocene deltaic sedimentation, Louisiana Gulf Coast, in Morgan, J. P., ed., Deltaic sedimentation, modern and ancient: Society of Economic Paleontologists and Mineralogists, p. 293-308.
- Dailly, G. C., 1976, A possible mechanism relating progradation, growth faulting, clay diapirism and overthrusting in a regressive sequence of sediments: Bulletin of Canadian Petroleum Geology, v. 24, p. 92-116.
- Dickinson, W. R., 1981, Plate tectonic evolution of the southern Cordilleran: Arizona Geological Society Digest, v. 14, p. 113-135.
- Dodge, M. M., and Posey, J. S., 1981, Structural cross sections, Tertiary formations, Texas Gulf Coast: The University of Texas at Austin, Bureau of Economic Geology Cross Sections.
- Dow, W. G., 1978, Petroleum source beds on continental slopes and rises: American Association of Petroleum Geologists Bulletin, v. 62, p. 1584-1606.
- Doyle, J. D., 1979, Depositional patterns of Miocene facies, middle Texas Coastal Plain: The University of Texas at Austin, Bureau of Economic Geology Report of Investigations No. 99, 28 p.
- DuBar, J. R., 1983, Miocene depositional systems and hydrocarbon resources: the Texas Coastal Plain: The University of Texas at Austin, Bureau of Economic Geology, report prepared for U.S. Geological Survey under contract no. 14-08-0001-G-707, 99 p.
- Echols, D. J., and Curtis, D. M., 1973, Paleontologic evidence for mid-Miocene refrigeration from subsurface marine shales, Louisiana Gulf Coast: Gulf Coast Association of Geological Societies Transactions, v. 23, p. 422-426.
- Fisher, W. L., Brown, L. F., Jr., Scott, A. J., and McGowen, J. H., 1969, Delta systems in the exploration for oil and gas, a research colloquium: The University of Texas at Austin, Bureau of Economic Geology Special Publication, 212 p.
- Fisk, H. N., 1944, Geological investigation of the alluvial valley of the lower Mississippi River: Mississippi River Commission, 78 p.
- Foote, R. Q., ed., 1984, Summary report on the regional geology, petroleum potential, environmental consideration for development, and estimates of undiscovered recoverable oil and gas resources of the United States Gulf of Mexico Continental Margin in the area of proposed oil and gas lease sales nos. 81 and 84: U.S. Geological Survey Open-File Report 84-339.
- Frazier, D. E., 1974, Depositional-episodes: their relationship to the Quaternary stratigraphic framework in the northwestern portion of the Gulf Basin: The University of Texas at Austin, Bureau of Economic Geology Geological Circular 74-1, 28 p.
- Galloway, W. E., 1976, Sediments and stratigraphic framework of the Copper River fan-delta, Alaska: Journal of Sedimentary Petrology, v. 46, p. 726-737.
- Galloway, W. E., Henry, C. D., and Smith, G. E., 1982a, Depositional framework, hydrostratigraphy, and uranium mineralization of the Oakville Sandstone (Miocene), Texas Coastal Plain: The University of Texas at Austin, Bureau of Economic Geology Report of Investigations No. 113, 51 p.
- Galloway, W. E., Hobday, D. K., and Magara, Kinji, 1982b, Frio Formation of the Texas Gulf Coast Basin—depositional systems, structural framework, and hydrocarbon origin, migration, distribution, and exploration potential: The University of Texas at Austin, Bureau of Economic Geology Report of Investigations No. 122, 78 p.
- , 1982c, Frio Formation of the Texas Gulf Coastal Plain: depositional systems, structural framework, and hydrocarbon distribution: American Association of Petroleum Geologists Bulletin, v. 66, no. 6, p. 649-688.
- Hoel, H. D., 1982, Goliad Formation of the South Texas Gulf Coastal Plain: regional genetic stratigraphy and uranium mineralization: The University of Texas at Austin, Master's thesis, 173 p.
- Huc, A. Y., and Hunt, J. M., 1980, Generation and migration of hydrocarbons in offshore South Texas Gulf Coast sediments: Geochimica et Cosmochimica Acta, v. 44, p. 1081-1089.



- Jackson, M. P. A., and Galloway, W. E., 1984, Structural and depositional styles of Gulf Coast Tertiary continental margins: application to hydrocarbon exploration: American Association of Petroleum Geologists, Continuing Education Course Note Series No. 25, 226 p.
- Keen, C. E., Beaumont, C., and Boutilier, R., 1981, Preliminary results from a thermo-mechanical model for the evolution of Atlantic-type continental margins: *Oceanologica Acta*, no. SP, p. 123-128.
- Kiatta, H. W., 1971, The stratigraphy and petroleum potential of the lower Miocene, offshore Galveston and Jefferson Counties, Texas: Gulf Coast Association of Geological Societies Transactions, v. 21, p. 257-270.
- Leckie, R. M., and Webb, P. N., 1983, Late Oligocene-early Miocene glacial record of the Ross Sea, Antarctica: evidence from DSDP, site 270: *Geology*, v. 11, p. 578-582.
- Loutit, T. S., and Kennett, J. P., 1981, Australasian Cenozoic sedimentary cycles, global sea-level changes and the deep sea sedimentary record: *Oceanologica Acta*, no. SP, p. 45-63.
- Martin, R. G., 1978, Northern and eastern Gulf of Mexico continental margin: stratigraphic and structural framework: American Association of Petroleum Geologists, Studies in Geology No. 7, p. 21-42.
- McDowell, F. W., and Clabaugh, S. E., 1979, Ignimbrites of the Sierra Madre Occidental and their relation to tectonic history of western Mexico: Geological Society of America Special Paper 1180, p. 113-124.
- Morton, R. A., Jirik, L. A., and Foote, R. Q., 1985a, Depositional history, facies analysis, and production characteristics of hydrocarbon-bearing sediments, offshore Texas: The University of Texas at Austin, Bureau of Economic Geology Geological Circular 85-2, 31 p.
- 1985b, Structural cross sections, Miocene Series, Texas continental shelf: The University of Texas at Austin, Bureau of Economic Geology Cross Sections.
- North American Commission on Stratigraphic Nomenclature, 1983, North American stratigraphic code: American Association of Petroleum Geologists Bulletin, v. 67, p. 841-875.
- Rainwater, E. H., 1964, Regional stratigraphy of the Gulf Coast Miocene: Gulf Coast Association of Geological Societies Transactions, v. 14, p. 81-124.
- Rice, D. J., 1980, Chemical and isotopic evidence of the origins of natural gases in offshore Gulf of Mexico: Gulf Coast Association of Geological Societies Transactions, v. 30, p. 203-213.
- Solis, R. F., 1981, Upper Tertiary and Quaternary depositional systems, central Coastal Plain, Texas—regional geology of the coastal aquifer and potential liquid-waste repositories: The University of Texas at Austin, Bureau of Economic Geology Report of Investigations No. 108, 89 p.
- Spradlin, S. D., 1980, Miocene fluvial systems: southeast Texas: The University of Texas at Austin, Master's thesis, 139 p.
- Stenzel, H. B., Turner, F. E., and Hesse, C. J., 1944, Brackish and non-marine Miocene in southeastern Texas: American Association of Petroleum Geologists Bulletin, v. 28, p. 977-1011.
- Tedford, R. H., and Hunter, M. E., 1984, Miocene marine-nonmarine correlations, Atlantic and Gulf coastal plains, North America: *Palaeogeography, Palaeoclimatology, Palaeoecology*, v. 47, p. 129-151.
- van Andel, T. J. H., 1967, The Orinoco delta: *Journal of Sedimentary Petrology*, v. 37, p. 297-310.
- Wallace, R. H., Jr., Wesselman, J. B., and Kraemer, T. F., 1981, Map of the occurrence of geopressure in the northern Gulf of Mexico, in Dorfman, M. H., and Fisher, W. L., eds., Proceedings, 5th U.S. Gulf Coast Geopressured-Geothermal Energy Conference: The University of Texas at Austin, Center for Energy Studies.
- Weeks, A. W., 1945, Balcones, Luling, and Mexia fault zones in Texas: American Association of Petroleum Geologists Bulletin, v. 29, p. 1733-1737.
- White, D. A., 1980, Assessing oil and gas plays in facies-cycle wedges: American Association of Petroleum Geologists Bulletin, v. 64, p. 1158-1178.
- Winker, C. D., 1979, Late Pleistocene fluvial-deltaic deposition, Texas Coastal Plain and Shelf: The University of Texas at Austin, Master's thesis, 187 p.
- 1982, Cenozoic shelf margins, northwestern Gulf of Mexico Basin: Gulf Coast Association of Geological Societies Transactions, v. 32, p. 427-448.
- Winker, C. D., and Edwards, M. B., 1983, Unstable progradational clastic shelf margins: Society of Economic Paleontologists and Mineralogists Special Publication No. 33, p. 139-157.

## APPENDIX: Tabulation of fields by play.

Accumulated production (through December 1982 in onshore fields and through June 1984 in offshore State tracts) assigned to lower Miocene reservoirs is also listed. Fields are located by identification (ID) number in figure 17. Asterisks indicate Federal OCS fields for which post-1979 production statistics have not been released.

### MIOCENE PRODUCTION DATA

ID No.	Field Name	Oil (10 <sup>6</sup> MMbbl)	Total Gas (10 <sup>6</sup> Mcf)	Condensate (10 <sup>6</sup> MMbbl)
<b>Play I</b>				
5	Holly Beach	0	108.0	0.2
6	Luttes	0	13.4	0
8	Parks Farm	0	12.7	0
9	Port Isabel West	0	25.5	0
10	San Martin	0	17.3	0
11	Three Islands East	0	23.3	<<0.1
12	Vista Del Mar	0	6.2	0
58	Arroyo Colorado	0	11.8	0
63	Paso Real	0	7.4	<0.1
	Total	0	225.6	~0.2
<b>Play IIa</b>				
26	Chevron	0	16.8	0.7
<b>Play IIb</b>				
-	-	-	-	-
<b>Play III</b>				
122	Brazos Block 386-S	0	66.0	0
122.5	Freeport Block 278	-	14.3	-
161	Galveston Block 310-L	0	28.1	0.2
213	Brazos Block 368-L	0	17.0	0
213.5	Middle Bank Reef	-	28.7	-
216	Brazos Block 405	0	111.1	0
217	Brazos Block 440	0	117.0	0
218	Brazos Block 445-G	0	25.8	<0.1
219	Brazos Block 446	0	42.9	0
220	Brazos Block 519-S	0	7.9	<<0.1
223	Cove	0	82.6	0
224	El Gordo	0	128.8	2
224.5	Cavallo	-	94.5	-
226	Kain	0	15.6	<<0.1
233	Sargent South	0	28.4	0
234	Matagorda Island Block 485-L	0	7.1	0
235	Matagorda Island Block 582-S	0	7.9	0
	Total	0	823.7	~2.2

## Appendix (cont.)

ID No.	Field Name	Oil (10 <sup>6</sup> MMbbl)	Total Gas (10 <sup>6</sup> Mcf)	Condensate (10 <sup>6</sup> MMbbl)
<b>Play IV</b>				
153	Block 176-S Miocene	0.2	11.1	0.1
153.5	Galveston Block 104-L	-	11.8	0.1
154	Brazos Block 255*	0.3	5.5	0.1
155.5	Brazos Block 98-L	-	15.3	<<0.1
157	Brazos Block 189*	0.8	0.6	0
160	Galveston Bay West	0	16.9	0.1
162	Galveston Island	0	68.2	0.2
165	Lafittes Gold	0.4	22.2	0.2
167	Shipwreck	0	105.1	0.4
167.5	Galveston Block 102-L	-	78.4	<<0.1
183	High Island Block 10-L	0.3	4.5	<0.1
183.5	Block 23-L	-	6.1	<<0.1
184	High Island Block 14-L	0	220.7	0.2
186	High Island Block 24-L	1.4	283.9	1
187	High Island Block 30 and 30-L	2.5	37.0	0.5
188	High Island Block 52-M*	1.9	42.0	0.4
190	High Island Block 140-L*	0	116.0	0.7
191	High Island Block 160*	0	348.0	0
198	High Island Block 88*	0	7.7	<<0.1
202	Sabine Pass	0.3	25.4	<0.1
Total		8.1	1,426.4	~4.1

## Play V

69	Jay Welder	1.1	0.4	<<0.1
70	Matagorda Bay	1.4	26.4	<<0.1
72	Powderhorn	4.3	7.3	0
73	Powderhorn South	0.2	20.3	<0.1
74	Saluria	0	11.0	0
76	Six-Sixty	0	18.0	0
221	College Port	0	53.7	<0.1
228	Matagorda Bay	0	51.2	0
229	Oliver Point	<<0.1	12.1	0
231	Oyster Lake West	<0.1	10.4	0
232	Rusty	0	3.1	0
Total		7.0	213.9	~0.1

# Appendix (cont.)

ID No.	Field Name	Oil (10 <sup>6</sup> MMbbl)	Total Gas (10 <sup>6</sup> Mcf)	Condensate (10 <sup>6</sup> MMbbl)
<b>Play VI</b>				
1	Fulton Beach	1.3	0	0
2	Half Moon Reef	0.7	9.2	0.1
14	Hidalgo West	0	16.3	0
15	Cabazos	0.4	6.1	<<0.1
22	Rita	0.7	97.2	<<0.1
23	San Jose	0	20.0	0
24	Sarita	8.6	148.0	0
25	Stillman	0	103.1	0
27	Alazan	5.0	26.2	0
28	Alazan North	4.2	62.8	0
29	Hinojosa	0.9	17.4	0
30	Kingsville	2.5	1.3	<<0.1
34	Baldwin	3.9	4.6	0
35	Clara Driscoll	8.1	4.0	0
36	Cody	2.4	2.1	0
37	Corpus Christi	6.8	2.5	0
39	London (aka London Gin)	20.7	1.0	0
40	Luby	9.9	5.4	0
42	Minnie Bock	10.8	0.2	0
43	Nueces Bay	1.1	7.3	<<0.1
45	Ramada	1.7	0.6	0
46	Saxet	31.3	7.8	0.1
47	Turkey Creek	4.3	0.2	0
48.5	Chapman Ranch	3.1	13.3	<<0.1
50	Plymouth	0.9	4.9	0
52	Reymer	0	12.4	0
55	Taft	19.9	3.7	0
56	Taft West	2.9	1.3	0
57	White Point	0.2	36.4	0
59	Chess	0.8	3.6	0.1
62	LaSara	2.4	6.2	<<0.1
64	Raymondville	0.9	8.7	<0.1
66	Willimar	48.7	0.1	0.3
68	Heyser	0	33.6	0
86	Granado	0	13.2	0
87	Hornberger	0	7.7	0
91	West Ranch	0	34.0	0
97	Fagan	0	23.0	0
98	Greta	1.3	32.0	0
99	Huff	0.6	27.8	0
100	La Rosa	0	6.2	0
101	Lake Pasture	0	225.5	0
102	Lake Pasture West	0	18.0	<<0.1
103	Refugio Heard	2.1	5.8	0
104	Refugio New	18.9	3.0	0
105	Refugio Old	4.5	3.0	0
106	Refugio Fox	22.1	0.5	0



## Appendix (cont.)

ID No.	Field Name	Oil (10 <sup>6</sup> MMbbl)	Total Gas (10 <sup>6</sup> Mcf)	Condensate (10 <sup>6</sup> MMbbl)
-----------	------------	--------------------------------	---------------------------------------	---------------------------------------

### Play VI (cont.)

107	Tom O'Connor	11.6	21.1	<<0.1
113	McFaddin	0	47.4	0
239	Blue Basin	0	15.9	0
241	Duffy	0	8.1	<<0.1
242	Hillje	2.6	3.6	<<0.1
245	Lane City	5.0	0.9	0
247	Louise	0	10.0	<<0.1
249	Magnet-Withers	13.4	109.0	<<0.1
252	Prasifka	0.9	6.6	0
	Total	285.5	1,289.8	~0.7

### Play VII

3	Alta Mesa	9.3	9.8	<0.1
33	Agua Dulce	0	9.7	0
49	Odern	0	6.6	0
53	Sinton North	2.1	1.0	0
54	Sinton West	5.7	5.1	0
79	Terrel Point	0	9.3	0
81	Collier	1.0	0.7	0
83	Cordele South	1.8	0.3	0
84	Cordele West	1.2	3.0	0
90	Navidad	0	7.1	0
108	Coletto Creek	12.5	2.9	0
109	Coletto Creek South	0	6.9	0
110	Cologne	0	17.7	0
116	Pridham Lake	2.2	4.4	0
117	Salem	0	13.9	0
118	Telferner	0.4	6.5	0
119	Victoria	1.5	1.0	0
244	Hutchins	0.3	9.4	<0.1
248	Louise North	0	18.4	0
250	New Taiton	0	28.0	0
251	Karstedt & Popp	0.0	18.5	0
253	Spanish Camp	0	252.1	0
254	Trans-Tex	0	30.4	0
255	Hungerford	0	9.2	0
	Total	38.0	471.9	<0.1

# Appendix (cont.)

ID No.	Field Name	Oil (10 <sup>6</sup> MMbbl)	Total Gas (10 <sup>6</sup> Mcf)	Condensate (10 <sup>6</sup> MMbbl)
<b>Play VIII</b>				
121	Bastrop Bay	1.1	2.6	<<0.1
124	Damon Mound	21.7	0.4	0
125	Danbury	18.8	6.6	<0.1
127	Hastings	321.8	33.1	<0.1
128	Hoskins Mound	7.5	4.4	0
129	Manvel	74.1	12.6	0
130	Nash Dome	5.0	2.2	0
131	Pledger	0.2	139.4	0.3
132	Rattlesnake Mound	0.2	6.7	<0.1
133	Stratton Ridge	3.7	0.1	0
134	West Columbia	125.2	0.8	0
136	Anahuac	0	27.4	<0.1
137	Barbers Hill	25.7	0.1	0
138	Cedar Point	11.0	1.7	<<0.1
139	Lost Lake	1.5	0.3	0
140	Red Fish Reef	0	14.9	<0.1
141	Winnie North	1.8	7.5	0.1
147	Big Creek	24.4	0.2	0
148	Blue Ridge	21.5	<<0.1	0
149	Moores Orchard	7.3	1.7	<<0.1
150	Needville	<0.1	27.4	<<0.1
151	Sugarland	70.9	1.6	0
152	Thompson	417.6	65.6	<<0.1
155	Caplen	17.6	15.8	0.1
156	Crystal Beach	<<0.1	1.3	<<0.1
163	High Island	88.4	0.9	0
164	Hitchcock	5.0	3.7	<0.1
166	Point Bolivar North	4.8	7.8	<0.1
169	Batson Old	44.2	<<0.1	0
170	Saratoga	19.4	0.1	0
171	Sour Lake	41.7	0.1	0
171.5	Arriola	6.3	0.5	0
173	Clinton	3.2	10.9	<<0.1
175	Dyersdale	19.1	1.5	0
176	Goose Creek	135.1	0.5	0
178	Humble	149.7	1.0	0
179	Olcott	0	20.5	0
180	Pierce Junction	21.1	0.1	0
182	Webster	133.8	27.2	0
192	Amelia	4.0	3.0	0
194	Beaumont West	20.1	9.1	<0.1
195	Big Hill	9.4	16.8	0.1
196	Clam Lake	18.9	0.5	0
197	Fannett	4.0	0.2	0
199	La Belle	12.1	5.9	<0.1
201	McFaddin Ranch	1.5	4.5	<<0.1

### Appendix (cont.)

ID No.	Field Name	Oil (10 <sup>6</sup> MMbbl)	Total Gas (10 <sup>6</sup> Mcf)	Condensate (10 <sup>6</sup> MMbbl)
-----------	------------	--------------------------------	---------------------------------------	---------------------------------------

### Play VIII (cont.)

203	Spindletop	102.2	0.2	0
204	Stowell	34.7	10.3	<0.1
205	Dayton North	1.4	<<0.1	0
206	Esperson	10.6	9.3	0
207	Hankamer	43.1	6.5	<0.1
210	Hull	91.2	1.0	0
211	Liberty South	13.3	0.4	0
212	Moss Bluff	1.5	<<0.1	0
227	Markham	17.7	0.1	0
237	Orange	61.5	0.6	0
238	Port Neches	18.9	0.3	0
240	Boling	24.3	<0.1	0
	Total	2,340.8	517.9	~1.1

### Play IX

13	Sejita East	0.3	8.0	0
92	Borchers	0	24.3	0
93	Hope	0	11.1	0
143	Garwood	0	11.3	0
145	Mustang Creek	0	10.3	0
174	Deckers Prairie South	0	11.0	0
181	Tomball	0	6.2	0
236	Conroe	0	7.4	<<0.1
246	Lissie	0	18.8	0
	Total	0.3	108.4	<<0.1





